
Adaptive Federated Learning with Auto-Tuned Clients

Junhyung Lyle Kim¹ Mohammad Taha Toghani² César A. Uribe² Anastasios Kyriallidis¹

¹Department of Computer Science ²Department of Electrical and Computer Engineering
Rice University

{jlylekim, mttoghani, cauribe, anastasios}@rice.edu

Abstract

Federated learning (FL) is a distributed machine learning framework where the global model of a central server is trained via multiple collaborative steps by participating clients without sharing their data. While being a flexible framework, where the distribution of local data, participation rate, and computing power of each client can greatly vary, such flexibility gives rise to many new challenges, especially in the hyperparameter tuning on both the server and the client side. We propose Δ -SGD, a simple step size rule for SGD that enables each client to use its own step size by adapting to the local smoothness of the function each client is optimizing. We provide theoretical and empirical results where the benefit of the client adaptivity is shown in various FL scenarios. In particular, our proposed method achieves TOP-1 accuracy in 73% and TOP-2 accuracy in 100% of the experiments considered without additional tuning.

1 Introduction

Federated learning (FL) is a distributed machine learning framework that allows multiple clients to learn a global model collaboratively. Each client trains the model on its local data and sends only the updated model parameters to a central server for aggregation. Mathematically, FL aims to solve the following optimization problem:

$$\min_{x \in \mathbb{R}^d} f(x) := \frac{1}{m} \sum_{i=1}^m f_i(x), \quad (1)$$

where $f_i(x) := \mathbb{E}_{z \sim \mathcal{D}_i}[F_i(x, z)]$ is the loss function of the i -th client, and m is the number of clients.

A key property of FL is its flexibility in *how different clients participate in the overall training*: the number of clients m , their participation rates, and computing power available to each client can all vary and change at any point during the overall training procedure. On top of that, each client’s local data is not shared with other clients or the server, resulting in certain inherent data privacy [35, 1].

While advantageous, such flexibility and data privacy also introduce a plethora of new challenges, notably: *i*) how the server aggregates the local information coming from each client, and *ii*) how to make sure each client meaningfully “learns” using their local data and computing device. The first challenge was partially addressed in [47], where adaptive optimization methods, such as Adagrad [13] or Adam [24], were utilized in the aggregation step. However, the second challenge remains largely unaddressed as we elaborate below, other than the exception of [57, 59] reviewed in Section 2.

Local data of each client is not shared, which intrinsically implies heterogeneity in terms of the size and the distribution \mathcal{D}_i of local datasets. That is, \mathcal{D}_i differs for each client i , as well as the number of samples $z \sim \mathcal{D}_i$. Consequently, $f_i(x)$ can vastly differ from client to client, making Problem (1) hard to solve (i.e., find an approximate minimizer). Moreover, the sheer amount of local updates is

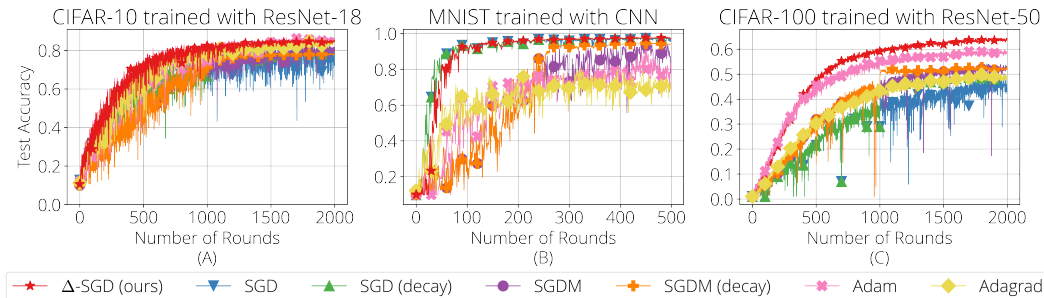


Figure 1: (A): CIFAR-10 classification task trained on ResNet-18. (B): MNIST classification task trained on shallow CNN. (C): CIFAR-100 classification task trained on ResNet-50. All experiments use FedAvg [35] as the server optimizer.

far larger than the number of aggregation steps, given that less communication is desired (i.e., less server-side aggregation) due to the high communication cost—typically $3\text{-}4\times$ orders of magnitude more expensive than local computation—in distributed optimization settings [27].

Extensive fine-tuning of the client optimizers is often required to achieve good performance. For instance, experimental results of the famous FedAvg algorithm were obtained after performing a grid-search of typically 11-13 step sizes of the clients’ SGD [35, Section 3], as SGD (and its variants) are highly sensitive to the step size [36, 52, 4, 23]. Similarly, in [47], 6 different client step sizes were grid-searched for different tasks, and not surprisingly, each task requires a different client step size to obtain the best result, regardless of the server-side adaptivity [47, Table 8]. Importantly, even these “fine-tunings” are done under the setting that *all clients use the same step size*, which is sub-optimal, given that f_i can be vastly different per client; we analyze this further in Section 2.

Initial examination as motivation. The implication of not properly tuning the client optimizer is highlighted in Figure 1. We plot the progress of test accuracies for different client optimizers, where, for all the other test cases, we intentionally use *the same step size rules that were fine-tuned for the task in Figure 1(A)*. There, we train a ResNet-18 for CIFAR-10 dataset classification within an FL setting, where the best step sizes were used for all algorithms after grid-search; we defer the experimental details to Section 4. Hence, all methods perform reasonably well, although Δ -SGD, our proposed method, achieves noticeably better test accuracy when compared to non-adaptive SGD variants—e.g., a 5% difference in final classification accuracy from SGDM— and comparable final accuracy only with adaptive SGD variants, like Adam and Adagrad.

In Figure 1(B), we train a shallow CNN for MNIST data classification using the same step size rules. MNIST classification is now considered an “easy” task, and therefore SGD with the same constant and decaying step sizes from Figure 1(A) works well. However, with momentum, SGDM exhibits highly oscillating behavior, which results in slow progress and poor final accuracy, especially without decaying the step size. Adaptive optimizers, like Adam and Adagrad, show similar behavior, falling short in achieving good final accuracy, compared to their performance in the case of Figure 1(A).

Similarly, in Figure 1(C), we plot the test accuracy progress for CIFAR-100 classification trained on ResNet-50, again using the same step size rules as before. Contrary to Figure 1(B), SGD with momentum (SGDM) works better than SGD, both with the constant and the decaying step sizes. Adam becomes a “good optimizer” again, but its “sibling”, Adagrad, performs worse than SGDM. On the contrary, our proposed method, Δ -SGD, which we introduce in Section 3, achieves superior performance in all cases without any additional tuning.

The above empirical observations beg answers to important and non-trivial questions in training FL tasks using variants of SGD methods as the client optimizer: *Should the momentum be used? Should the step size be decayed? If so, when?* Unfortunately, Figure 1 indicates that the answers to these questions highly vary depending on the setting; once the dataset itself or how the dataset is distributed among different clients changes, or once the model architecture changes, the client optimizers have to be properly re-tuned to ensure good performance. Perhaps surprisingly, the same holds for adaptive methods like Adagrad [13] and Adam [24].

Our hypothesis and contributions. Our paper takes a stab in this direction: we propose DELTA-SGD (DistributEd LocaliTy Adaptive SGD), a simple adaptive SGD scheme, that does not require any knowledge of the problem constants, such as the L -smoothness parameter. We will refer to our algorithm as Δ -SGD in the rest of the text. Our adaptive step size is extended from [34], where

the focus was centralized convex optimization; we defer the readers to Section 3 for details. Our contributions can be summarized as follows:

- We extend the (centralized) adaptive step size from [34] to the FL setting. The implication of this adaptive step size in FL is twofold: *i*) each client can use its own step size, and *ii*) each client’s step size *adapts to the local smoothness of f_i* —hence LocaliTy Adaptive— and can even *increase* during local iterations. Moreover, thanks to the simplicity of the proposed step size, our method is *agnostic to the server optimizer as well as the loss function*, and thus can be easily combined with server adaptive methods such as FedAdam [47], or methods that use different (regularized) loss functions such as FedProx [31] or MOON [30].
- We provide convergence analysis of Δ -SGD in a general nonconvex setting (Theorem 1). We also provide the convergence analysis in the convex setting, extending the analysis from [34] to a distributed one, as well as a simple centralized nonconvex convergence analysis, which was an open question posed in [34]. Due to space constraints, we only state the result of general nonconvex case in Theorem 1, and defer other theorems and proofs to Appendix A.
- We evaluate our approach on several benchmark datasets and demonstrate that Δ -SGD achieves superior performance compared to other state-of-the-art FL methods. Our experiments show that our method can effectively adapt the client step size to the underlying data distribution and achieve faster convergence of the global model, *without any additional tuning*. Our approach can help overcome the client step size tuning challenge in FL and enable more efficient and effective collaborative learning in distributed systems.

2 Preliminaries and Related Work

A bit of background on optimization theory. Arguably the most fundamental optimization algorithm for minimizing a function $f(x) : \mathbb{R}^d \rightarrow \mathbb{R}$ is the gradient descent (GD) [8], which iterates with the step size η_t as: $x_{t+1} = x_t - \eta_t \nabla f(x_t)$. Under the assumption that f is *globally L -smooth*, that is:

$$\|\nabla f(x) - \nabla f(y)\| \leq L \cdot \|x - y\| \quad \forall x, y, \quad (2)$$

the step size $\eta_t = \frac{1}{L}$ is the “optimal” step size for GD, which converges at the rate, which is not improvable [37, 12], for convex f :

$$f(x_{t+1}) - f(x^*) \leq \frac{L\|x_0 - x^*\|^2}{2(2t + 1)}, \quad (3)$$

while $\eta_t \in (0, \frac{2}{L})$ defines the “admissible” step size range required to ensure that GD converges for this function class [43]. Similarly, if f is also (globally) μ -strongly convex, that is:

$$f(x) \geq f(y) + \langle \nabla f(y), x - y \rangle + \frac{\mu}{2} \|x - y\|^2 \quad \forall x, y,$$

then the optimal step size is $\eta_t = \frac{2}{\mu + L}$ [37], and the rate improves to a linear one:

$$\|x_{t+1} - x^*\|^2 \leq \left(\frac{L - \mu}{L + \mu} \right)^t \|x_0 - x^*\|^2.$$

Limitations of popular step sizes. In practice, however, the constants L and μ are rarely known [7]. As such, there has been a plethora of efforts in the optimization community to come up with a general step size rule or method that does not require a priori knowledge of problem constants [38, 40, 29], so that an optimization algorithm can work as “plug-and-play.”

This is a well-known research question, with some major lines of work on this direction being: *i*) line-search [2, 41], *ii*) adaptive learning rate (e.g., Adagrad [13] and Adam [24]), and *iii*) Polyak step size [44, 17], to name a few. Unfortunately, the search for the “perfect” step size is still active [33, 11, 10, 5, 28], as the aforementioned approaches have limitations. For instance, to use line search, solving a sub-routine is often required, inevitably incurring additional evaluations of the function and/or the gradient. To use methods like Adagrad and Adam, the knowledge of the initial distance from the solution set D , which is nontrivial to find, is required to ensure good performance [10]; see also Section 4. Lastly, Polyak step size requires a sharp knowledge of $f(x^*)$ [17], which is not always known a priori, and is unclear what value to use for an arbitrary loss function and model.

Implications in FL scenarios. On top of that, even with the knowledge of L , GD can be slow. Indeed, the global L -smoothness condition, as described above, needs to be satisfied for all x and

y , implying even finite L can be arbitrarily large. This results in a small step size, leading to slow convergence, as seen in (3).

Naturally, the challenge is aggravated in the distributed case. To solve (1), under the assumption that each f_i is L_i -smooth, the step size of the form $1/L_{\max}$ where $L_{\max} := \max_i L_i$ is often used [62, 48, 46], to ensure convergence [53]. Yet, one can easily imagine a situation where $L_i \gg L_j$ for $i \neq j$, in which case the convergence of $f_j(x)$ can be arbitrarily slow by using step size $1/L_{\max}$.

There are plenty of practical examples where such a scenario could happen. For instance, imagine smartphone photo albums of the members of a fishing club versus a bird-watching club. The albums of these two groups could have vastly different data distributions, one skewed with pictures including fishes and rivers, while the other skewed with birds and forests [56]. On top of that, smartphones from different manufacturers nowadays have distinctly different camera filters applied—recently a big selling point for companies like Apple, introducing technologies like “portrait mode,” and Samsung, introducing 100× zoom capability, both based on image processing techniques—making even similar pictures to have distinct pixel values, when taken with different smartphones.

Therefore, to ensure that each client learns useful information in the FL setting as in (1), ideally: *i*) each agent should be able to use its own step size, instead of crude ones like $1/L_{\max}$ for all; *ii*) the individual step size should be “locally adaptive” to the function f_i , (i.e., even $1/L_i$ can be too crude, analogously to the centralized GD); and *iii*) the step size should not depend on problem constants like L_i or μ_i , which are often unknown. In Section 3, we introduce **DistributEd LocaliTy Adaptive SGD** (Δ -SGD), which satisfies all of the aforementioned desiderata.

Related work on FL. FedAvg [35] is the simplest and probably the most famous FL algorithm, which takes a (weighted) average of the client parameters in the aggregation step after clients perform some local iterations. While FedAvg has achieved great results empirically, it has been observed recently that it can suffer from model drift [45] induced by the heterogeneity [19]. At the core, simple averaging is too crude of an operation. As such, FedAvg uses a weighted average heuristic, where the weights are based on the number of data n_i for each client i [35].

The authors in [47] took this idea one step further: it showed that FedAvg can be seen as a special case where both the clients and the server use the SGD optimizer, with a server learning rate of 1. To handle the heterogeneity and the model drift, they proposed to use adaptive optimization scheme *at the server*, resulting in, e.g., FedAdam or FedYogi, which respectively use Adam [24] and Yogi [63] as the server optimizer, and can improve upon FedAvg in various scenarios. Note that this fundamentally differs from our approach, where *we propose a client adaptive optimizer that can be easily combined with sophisticated server-side aggregation methods like FedAdam*.

Perhaps the closest works in spirit to our work are AdaAlter [59] and locality adaptivity in FL [57]. Both works utilize an adaptive client optimizer, similar to Adagrad [13], with either delayed or restarted updates on the adaptive variables (e.g., pre-conditioners and momentum buffers). However, as noted in [47], AdaAlter incurs twice the memory compared to FedAvg, as AdaAlter requires communicating both the model parameters as well as the “client accumulators,” which is of the same dimension as model parameters. [57] overcomes this issue by simply restarting the client optimizer states, but requires complicated local *and* global correction step to achieve good performance. On the contrary, Δ -SGD changes virtually nothing compared to FedAvg other than the simple step size computation, and yet still achieves impressive performance; see Section 4.

Other approaches have handled the heterogeneity by changing the loss function. FedProx [31] adds an ℓ_2 -norm proximal term to the individual loss functions such that the local parameters do not diverge too much from the previously communicated global model. Similarly, MOON [30] uses the cross-entropy loss between the current and previous models. As mentioned in the introduction, our proposed method can be seamlessly combined with these approaches.

Another line of works attempts to handle heterogeneity by utilizing control-variates [45, 32, 21], a similar idea to variance reduction from single-objective optimization [20, 16]. While theoretically appealing, these methods either require full gradient computation periodically or are not usable when not all the clients participate, as the clients must maintain a state throughout all rounds.

3 DELTA(Δ)-SGD: Distributed locality adaptive SGD

In [34], a novel step size rule for (centralized) GD was introduced, which adapts to the minimization function’s local geometry. The proposed step size is clever and strikingly simple:

$$\eta_t = \min \left\{ \frac{\|x_t - x_{t-1}\|}{2\|\nabla f(x_t) - \nabla f(x_{t-1})\|}, \sqrt{1 + \theta_{t-1}\eta_{t-1}} \right\}, \quad \theta_{t-1} = \eta_{t-1}/\eta_{t-2}. \quad (4)$$

The step size in (4) adapts to the *local smoothness* of the iterates, that is:

$$\|\nabla f(x_t) - \nabla f(x_{t-1})\| \leq L_t \cdot \|x_t - x_{t-1}\|, \quad \forall t = 1, 2, \dots \quad (5)$$

and hence can *increase during iterations*, while the second condition in (4) ensures that η_t does not increase arbitrarily. By definition, L_t in (5) is never bigger than the global L in (2), resulting in faster convergence in practice [34, Section 4]. Note that (4) is vastly different from some standard adaptive methods like Adagrad [13], which can only decrease the learning rate, as they accumulate non-negative quantities in the denominator of the step size. As a result, the scalar multiplied to their “adaptive” learning rates play a crucial role and requires proper tuning, similarly to vanilla SGD, as evident in Figure 1; see also Table 1 in Section 4.

We now introduce DELTA(Δ)-SGD: DistributEd LocaliTy Adaptive SGD, where we extend (4) to the FL setting, with the inclusion of stochasticity and local iterations, as summarized in Algorithm 1. For brevity, we use $\tilde{\nabla} f_i(x) = \frac{1}{|\mathcal{B}|} \sum_{z \in \mathcal{B}} F_i(x, z)$ to denote the stochastic gradients with batch size $|\mathcal{B}| = b$.

Algorithm 1 DELTA(Δ)-SGD: DistributEd LocaliTy Adaptive SGD

```

1: input:  $x_0 \in \mathbb{R}^d$ ,  $\eta_0, \theta_0, \gamma > 0$ , and  $p \in (0, 1)$ .
2: for each round  $t = 0, 1, \dots, T-1$  do
3:   sample a subset  $\mathcal{S}_t$  of clients with size  $|\mathcal{S}_t| = p \cdot m$ 
4:   for each machine in parallel for  $i \in \mathcal{S}_t$  do
5:     Set  $x_{t,0}^i = x_t$ 
6:     Set  $\eta_{t,0}^i = \eta_0$  and  $\theta_{t,0}^i = \theta_0$ 
7:     for local step  $k \in [K]$  do
8:        $x_{t,k}^i = x_{t,k-1}^i - \eta_{t,k-1}^i \tilde{\nabla} f_i(x_{t,k-1}^i)$  ▷ update local parameter with  $\Delta$ -SGD
9:        $\eta_{t,k}^i = \min \left\{ \frac{\gamma \|x_{t,k}^i - x_{t,k-1}^i\|}{2\|\tilde{\nabla} f_i(x_{t,k}^i) - \tilde{\nabla} f_i(x_{t,k-1}^i)\|}, \sqrt{1 + \theta_{t,k-1}^i \eta_{t,k-1}^i} \right\}$ 
10:       $\theta_{t,k}^i = \eta_{t,k}^i / \eta_{t,k-1}^i$  ▷ (line 10 & 11) update locality adaptive step size
11:     end for
12:   end for
13:    $x_{t+1} = \frac{1}{|\mathcal{S}_t|} \sum_{i \in \mathcal{S}_t} x_{t,K}^i$  ▷ server-side aggregation
14: end for
15: return  $x_T$ 

```

We make a few remarks about Algorithm 1. First, the input $\eta_0 > 0$ can be quite arbitrary, as it can be corrected, per client level, in the 1st local iteration (line 9); similarly for $\theta_0 > 0$ (line 10). Second, as the step size $\eta_{t,k}^i$ requires two successive stochastic gradients, there could be two options: using *i*) the same batch or *ii*) a new batch; the second option will incur additional memory requirement, so we use the first.¹ Third, we include the “amplifier” γ to the first condition of step size (line 9), but this is only needed for Theorem 1.² fourth, after local steps are done, η_0 is re-used (line 6); we could potentially use a more sophisticated approach and use a similar adaptive step size to line 9, but we leave this for future work. Last, we present simple averaging as the server-side aggregation for simplicity (line 13), but more sophisticated methods like FedAdam [47] can be used instead.

¹This distinction was already analyzed in the centralized setting, and it was reported that using the same batch performed better in practice [34].

²In practice, we did not change from the default value $\gamma = 2$ in the original implementation in https://github.com/ymlitsky/adaptive_GD/blob/master/pytorch/optimizer.py.

3.1 Convergence Analysis

Technical challenges. Before we present the convergence analysis, let us elaborate on the non-trivial technical challenges of analyzing Algorithm 1. The main difference of analyzing Algorithm 1 compared to other distributed/decentralized optimization theory is that the step size $\eta_{t,k}^i$ not only depends on the round t and local steps k (which is a challenge shared by other analyses), *but also on i* , the client. To deal with the client-dependent step size, we require a slightly non-standard assumption on the dissimilarity between f and f_i , as shown below.

Assumption 1. *There exist nonnegative constants σ, ρ , and G such that for all $i \in [M]$ and $x \in \mathbb{R}^d$,*

$$\mathbb{E}\|\nabla F_i(x, z) - \nabla f_i(x)\| \leq \sigma^2, \quad (\text{bounded variance}) \quad (1a)$$

$$\|\nabla f_i(x)\| \leq G, \quad (\text{bounded gradient}) \quad (1b)$$

$$\|\nabla f_i(x) - \nabla f(x)\|^2 \leq \rho \|\nabla f(x)\|^2. \quad (\text{strong growth of dissimilarity}) \quad (1c)$$

Assumption 1a has been standard in stochastic optimization literature [36, 14, 50, 22]; recently, this assumption has been relaxed to weaker ones such as weak growth assumption [6] or expected smoothness [15], but this is out of scope of this work. Assumption 1b is fairly standard in nonconvex optimization [63, 58], and often used in FL setting [59, 60, 47]. Assumption 1c is reminiscent of the strong growth assumption in stochastic optimization literature [49], which is still used in recent works [9, 54, 55]. To the best of our knowledge, this is the first theoretical analysis of the FL setting where clients can use their step size. We now present the main convergence theorem of Algorithm 1.

Theorem 1. *Let Assumption 1 hold, with $\rho = \mathcal{O}(1)$. Further, suppose that $\gamma = \mathcal{O}(\frac{1}{K\sqrt{T}})$, and $\eta_0 = \mathcal{O}(\gamma)$. Then, the following property holds for Algorithm 1, for T sufficiently large:*

$$\frac{1}{T} \sum_{t=0}^{T-1} \mathbb{E} \|\nabla f(x_t)\|^2 \leq \mathcal{O}\left(\frac{\Psi_1}{\sqrt{T}}\right) + \mathcal{O}\left(\frac{\tilde{L}^2 \Psi_2}{T}\right) + \mathcal{O}\left(\frac{\tilde{L}^3 \Psi_2}{\sqrt{T^3}}\right),$$

where $\Psi_1 = \max\left\{\frac{\sigma^2}{b}, f(x_0) - f(x^*)\right\}$ and $\Psi_2 = \left(\frac{\sigma^2}{b} + G^2\right)$ are global constants, with $b = |B|$ being the batch size; \tilde{L} is a constant at most the average of local smoothness, i.e., $\max_t \frac{1}{m} \sum_{i=1}^m L_{i,t}$, where $L_{i,t}$ the local smoothness of f_i at round t .

The convergence result in Theorem 1 implies a sublinear convergence to an ε -first order stationary point with at least $T = \mathcal{O}(\varepsilon^{-2})$ communication rounds. We emphasize again that the conditions on γ and η_0 are only required for our theory.³ Importantly, we did not assume f_i is L -smooth (or even L_i -smooth), a standard assumption in nonconvex optimization and FL literature [58, 25, 31, 47]; instead, we can obtain a smaller quantity, \tilde{L} , through our analysis in a similar vein to (5); for space limitation, we defer the details and the proof to Appendix A.

4 Experimental Setup and Results

Datasets and models. To test the performance of different client optimizers in various settings, we evaluate on four datasets commonly used in FL scenarios: MNIST, FMNIST, CIFAR-10, and CIFAR-100 [26]. For MNIST and FMNIST, we train a shallow CNN with two convolutional and two fully-connected layers, followed by dropout and ReLU activations. For CIFAR-10, we train a ResNet-18 [18]. For CIFAR-100, we train both a ResNet-18 and a ResNet-50 to study the effect of changing the model architecture.

For each dataset, we create a federated version by randomly partitioning the training data among 100 clients, with each client getting 500 examples.⁴ To control the level of “non-iidness”, we apply latent Dirichlet allocation (LDA) over the labels following [19], where each client has an associated multinomial distribution over the labels from which its examples are drawn. That is, the local training examples of each client has been drawn from a categorical distribution over N classes, parameterized by \mathbf{q} , such that $\mathbf{q} \sim \text{Dir}(\alpha \mathbf{p})$, where \mathbf{p} is a prior distribution over N classes, with $\alpha > 0$ being the concentration parameter. We vary $\alpha \in \{0.01, 0.1, 1\}$, where bigger α indicates settings closer to i.i.d. scenarios. The class distribution of different α ’s is visualized in Figure 5 in Appendix B.

³In all experiments in Section 4, we use the default setting $\gamma = 2$, and $\eta_0 = 0.2$, without additional tuning.

⁴All the datasets we consider have 50,000 training samples, leading to 500 samples distributed per client.

FL setup and optimizers. For all cases, we fix the number of clients to be 100, and randomly sample 10% among the 100 clients. Similarly to [47, 31], we perform E local epochs of training over each client’s dataset, and we utilize mini-batch gradients of size $b = 64$, leading to $K \approx \lfloor \frac{E \cdot 500}{64} \rfloor$ local gradient steps; we use $E = 1$ for all settings. For client optimizers, we compare stochastic gradient descent (SGD), SGD with momentum (SGDM), adaptive methods including Adam [24], Adagrad [13], SGD with stochastic Polyak step size (SPS) [33], and our proposed method: Δ -SGD in Algorithm 1. As our focus is on client adaptivity, we only present the results using simple FedAvg [35] as the server optimizer.

Hyperparameters. For all methods, we perform a simple grid search on a *single task*: CIFAR-10 classification trained with ResNet-18, with Dirichlet concentration parameter $\alpha = 0.1$; for the rest of the settings, we use the same hyperparameters. For SGD, we perform a grid search with $\eta \in \{0.01, 0.05, 0.1, 0.5\}$. For SGDM, we use the same grid for η and use momentum parameter $\beta = 0.9$. For Adam, we tried $\eta \in \{0.001, 0.01\}$, and for Adagrad, we tried $\eta \in \{0.01, 0.1\}$ (i.e., the default learning rates in Pytorch and their one-tenths). For SPS, we use the default setting of the official implementation.⁵ For Δ -SGD, we append δ in front of the second condition: $\sqrt{1 + \delta \theta_{t,k-1}^i \eta_{t,k-1}^i}$ following [34], and use $\delta = 0.1$ for all experiments (however, as shown in Figure 4 in Appendix B, δ has little impact on final accuracy in most cases). To account for the SGD(M) fine-tuning done in practice, we also tested dividing the step size (LR decay) by 10 after 50%, and then again by 10 after 75% of the total training rounds and report the inclusive results in Table 1. Finally, for the number of rounds T , we use 500 for MNIST, 1000 for FMNIST, and 2000 for CIFAR-10 and CIFAR-100.

Implementation. We use Pytorch [42] to implement all experiments and run on eight P100 GPUs. Our implementation will be available online after the anonymous review process for reproducibility.

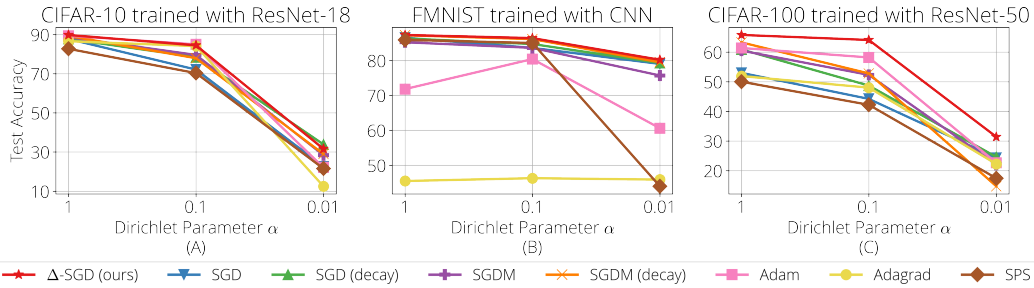


Figure 2: The effect of stronger heterogeneity on different client optimizers, induced by the Dirichlet concentration parameter α .

4.1 Results

Results of the experiments detailed in the previous subsection are presented in Table 1. Below, we make comprehensive remarks, depending on: *i*) the level of heterogeneity induced by different α ’s of the Dirichlet concentration parameter, *ii*) the effect of changing the model architecture, and *iii*) the effect of changing the dataset, and how these affect the performance of different client optimizers.

Changing the level of non-iidness. We first investigate how the performance of different client optimizers degrade in increasing degrees of heterogeneity by varying the concentration parameter $\alpha \in \{1, 0.1, 0.01\}$ multiplied to the prior of Dirichlet distribution, following [19].

Three illustrative cases are visualized in Figure 2. We remind that the hyperparameters are tuned for the case of CIFAR-10 trained with ResNet-18, with $\alpha = 0.1$ (Figure 2(A)). For this task, with $\alpha = 1$ (i.e., closer to iid), all methods perform better than $\alpha = 0.1$, as expected. With $\alpha = 0.01$, which is highly non-iid (c.f., Figure 5 in Appendix B), we see a significant drop in performance for all methods. SGD with LR decay and Δ -SGD perform the best, while adaptive methods like Adam (85% \rightarrow 22.1%) and Adagrad (84.1% \rightarrow 12.5%) degrade noticeably more than other methods.

For FMNIST trained with CNN (Figure 2(B)), which can be considered as an easier problem compared to CIFAR-10 classification, the performance degradation with varying α ’s is much milder.

⁵I.e., we use $f_i^* = 0$, an $c = 0.5$, for the SPS step size: $\frac{f_i(x) - f_i^*}{c \|\nabla f_i(x)\|^2}$. The official implementation can be found in <https://github.com/IssamLaradji/sps>

Non-iidness	Optimizer	Dataset / Model					
		MNIST CNN	FMNIST CNN	CIFAR-10 ResNet-18	CIFAR-100 ResNet-18	CIFAR-100 ResNet-50	
$\alpha = 1$	SGD	98.3 _{↓(0.2)}	86.5 _{↓(0.8)}	87.7 _{↓(2.1)}	57.7 _{↓(4.2)}	53.0 _{↓(12.8)}	
	SGD (↓)	97.8 _{↓(0.7)}	86.3 _{↓(1.0)}	87.8 _{↓(2.0)}	61.9 _{↓(0.0)}	60.9 _{↓(4.9)}	
	SGDM	98.5 _{↓(0.0)}	85.2 _{↓(2.1)}	88.7 _{↓(1.1)}	58.8 _{↓(3.1)}	60.5 _{↓(5.3)}	
	SGDM (↓)	98.4 _{↓(0.1)}	87.2 _{↓(0.1)}	89.3 _{↓(0.5)}	61.4 _{↓(0.5)}	63.3 _{↓(2.5)}	
	Adam	94.7 _{↓(3.8)}	71.8 _{↓(15.5)}	89.4 _{↓(0.4)}	55.6 _{↓(6.3)}	61.4 _{↓(4.4)}	
	Adagrad	64.3 _{↓(34.2)}	45.5 _{↓(41.8)}	86.6 _{↓(3.2)}	53.5 _{↓(8.4)}	51.9 _{↓(13.9)}	
	SPS	10.1 _{↓(88.4)}	85.9 _{↓(1.4)}	82.7 _{↓(7.1)}	1.0 _{↓(60.9)}	50.0 _{↓(15.8)}	
	Δ -SGD	98.4 _{↓(0.1)}	87.3 _{↓(0.0)}	89.8 _{↓(0.0)}	61.5 _{↓(0.4)}	65.8 _{↓(0.0)}	
	$\alpha = 0.1$	SGD	98.1 _{↓(0.0)}	83.6 _{↓(2.8)}	72.1 _{↓(12.9)}	54.4 _{↓(6.7)}	44.2 _{↓(19.9)}
		SGD (↓)	98.0 _{↓(0.1)}	84.7 _{↓(1.7)}	78.4 _{↓(6.6)}	59.3 _{↓(1.8)}	48.7 _{↓(15.4)}
		SGDM	97.6 _{↓(0.5)}	83.6 _{↓(2.8)}	79.6 _{↓(5.4)}	58.8 _{↓(2.3)}	52.3 _{↓(11.8)}
		SGDM (↓)	98.0 _{↓(0.1)}	86.1 _{↓(0.3)}	77.9 _{↓(7.1)}	60.4 _{↓(0.7)}	52.8 _{↓(11.3)}
		Adam	96.4 _{↓(1.7)}	80.4 _{↓(6.0)}	85.0 _{↓(0.0)}	55.4 _{↓(5.7)}	58.2 _{↓(5.9)}
		Adagrad	89.9 _{↓(8.2)}	46.3 _{↓(40.1)}	84.1 _{↓(0.9)}	49.6 _{↓(11.5)}	48.0 _{↓(16.1)}
SPS		96.0 _{↓(2.1)}	85.0 _{↓(1.4)}	70.3 _{↓(14.7)}	42.2 _{↓(18.9)}	42.2 _{↓(21.9)}	
Δ -SGD		98.1 _{↓(0.0)}	86.4 _{↓(0.0)}	84.5 _{↓(0.5)}	61.1 _{↓(0.0)}	64.1 _{↓(0.0)}	
$\alpha = 0.01$	SGD	96.8 _{↓(0.7)}	79.0 _{↓(1.2)}	22.6 _{↓(11.3)}	30.5 _{↓(1.3)}	24.3 _{↓(7.1)}	
	SGD (↓)	97.2 _{↓(0.3)}	79.3 _{↓(0.9)}	33.9 _{↓(0.0)}	30.3 _{↓(1.5)}	24.6 _{↓(6.8)}	
	SGDM	77.9 _{↓(19.6)}	75.7 _{↓(4.5)}	28.4 _{↓(5.5)}	24.8 _{↓(7.0)}	22.0 _{↓(9.4)}	
	SGDM (↓)	94.0 _{↓(3.5)}	79.5 _{↓(0.7)}	29.0 _{↓(4.9)}	20.9 _{↓(10.9)}	14.7 _{↓(16.7)}	
	Adam	80.8 _{↓(16.7)}	60.6 _{↓(19.6)}	22.1 _{↓(11.8)}	18.2 _{↓(13.6)}	22.6 _{↓(8.8)}	
	Adagrad	72.4 _{↓(25.1)}	45.9 _{↓(34.3)}	12.5 _{↓(21.4)}	25.8 _{↓(6.0)}	22.2 _{↓(9.2)}	
	SPS	69.7 _{↓(27.8)}	44.0 _{↓(36.2)}	21.5 _{↓(12.4)}	22.0 _{↓(9.8)}	17.4 _{↓(14.0)}	
	Δ -SGD	97.5 _{↓(0.0)}	80.2 _{↓(0.0)}	31.6 _{↓(2.3)}	31.8 _{↓(0.0)}	31.4 _{↓(0.0)}	

Table 1: Experimental results based on the settings detailed in Section 4. Performance difference within 0.5% of the best result for each task are shown in **bold**. Subscripts_{↓(x.x)} is the performance difference from the best result and is highlighted in **pink** when the difference is bigger than 2%. The symbol (↓) appended to SGD and SGDM indicates step-wise learning rate decay, where the step sizes are divided by 10 after 50%, and another by 10 after 75% of the total rounds.

Interestingly, adaptive methods like Adam, Adagrad, and SPS perform much worse than other methods, indicating their inflexibility when applied to diverse datasets and model architectures, which often is worse than simple SGD-based methods; we further investigate this phenomenon in more detail in the next remark.

A similar trend can be seen in MNIST classification, where SGD-based methods work relatively well, except for SGDM with $\alpha = 0.01$: without the LR decay, SGDM only achieves around 78% accuracy, while SGD without LR decay still achieves over 96% accuracy (c.f., Figure 1(A)). Even with the LR decay, SGDM achieves noticeably worse performance. While this may seem like an “easy fix” in hindsight, it indicates that in a highly non-iid setting, one should be extremely careful in tuning SGD-based methods, even for easy datasets like MNIST. Interestingly, SPS performs particularly poorly, merely achieving 10% for MNIST with $\alpha = 1$, while achieving 96% for “harder” case of $\alpha = 0.1$, and again dropping to 69.7% with $\alpha = 0.01$; a possible explanation is, with simple CNN, the model is not over-parameterized enough to have $f_i^* = 0$, the default estimate we use on which the performance of SPS crucially rely [17]. Adagrad similarly performs quite poorly.

Lastly, in Figure 2(C), results for CIFAR-100 classification trained with ResNet-50 are illustrated. Δ -SGD exhibits superior performance in all cases of α . Unlike MNIST and FMNIST, Adam enjoys the second ($\alpha = 0.1$) or the third ($\alpha = 1$) best performance in this task, complicating how one should “tune” Adam for the task at hand. Other methods, including SGD with and without momentum/LR decay, Adagrad, and SPS, perform much worse than Δ -SGD.

Changing the model architecture. For this remark, let us focus on CIFAR-100 trained on ResNet-18 versus on ResNet-50, with $\alpha = 0.1$, illustrated in Figure 3(A). SGD and SGDM (both with and without LR decay), Adagrad, and SPS perform worse using ResNet-50 than ResNet-18. This is a counter-intuitive behavior, as one would expect to get better accuracy by using a more powerful model. Δ -SGD is an exception: without any additional tuning, Δ -SGD can improve its performance. Adam also improves similarly, but the achieved accuracy is significantly worse than that of Δ -SGD. While it is true that the performance of Δ -SGD also slightly degrades for $\alpha = 0.01$, it still performs better than the other methods.

Changing the dataset. We now focus on cases where the dataset changes, but the model architecture remains the same. We mainly consider two cases, illustrated in Figure 3(B) and (C): When CNN is trained for classifying MNIST versus FMNIST, and when ResNet-18 is trained for CIFAR-10 versus CIFAR-100. Aggravating the complexity of fine-tuning SGD(M) for MNIST, one can observe a similar trend in CIFAR-10 trained with ResNet-18. In that case, Δ -SGD does not achieve the best test accuracy (although it is the second best with a pretty big margin with the rest), while SGD with LR decay does. However, without LR decay, the accuracy achieved by SGD drops more than 11%.

Interestingly, for the same setting, when we change the dataset from CIFAR-10 to CIFAR-100, SGD without LR decay (which is not one of the best methods for the CIFAR-10 case) achieves the second-best performance (after Δ -SGD). On the other hand, SGDM with LR decay, which achieves the 3rd best performance for CIFAR-10 achieves very poor performance (more than 10% less than the best) for CIFAR-100. Finally, SGD with decay, which performs the best in the CIFAR-10 case, turns out to be the 3rd best algorithm when we change the dataset to CIFAR-100. Again, adaptive methods like Adam, Adagrad, and SPS perform quite poorly in this case.

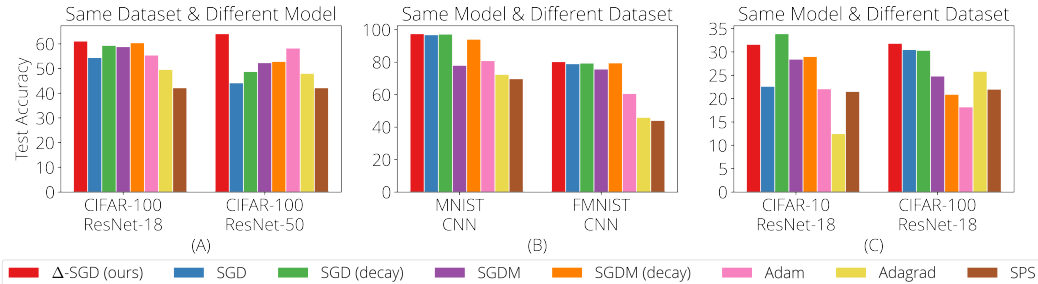


Figure 3: The effect of changing the dataset and the model architecture on different client optimizers. (A): CIFAR-100 trained with ResNet-18 versus Resnet-50 ($\alpha = 0.1$), (B): MNIST versus FMNIST trained with CNN ($\alpha = 0.01$), (C): CIFAR-10 versus CIFAR-100 trained with ResNet-18 ($\alpha = 0.01$).

5 Conclusion

In this work, we propose Δ -SGD, a distributed SGD scheme equipped with an adaptive step size that enables each client to use its step size and adapts to the local smoothness of the function each client is optimizing. We prove the convergence of Δ -SGD in the general nonconvex setting and present extensive empirical results, where the superiority of Δ -SGD is shown in various scenarios without any tuning. For future works, extending Δ -SGD to a coordinate-wise step size in spirit of [13, 24], as well as enabling asynchronous updates [3, 51, 39] could be interesting directions.

Broader Impacts and Limitations. We believe our proposed method, Δ -SGD, can potentially impact reducing the amount of tuning required in training FL models. By now, it is widely believed that FL systems do not “dodge the bullet” of high carbon emission in AI/ML: as noted in a recent study [61], “compute on client devices, and the communication between the clients and the server are responsible for the majority of FL’s overall carbon emissions (97%).” The lack of principled hyperparameter tuning only exacerbates this problem. Based on the results presented in Section 4, Δ -SGD achieves superior performance while robust to different settings.

In terms of limitations, our assumption on Theorem 1, especially Assumption 1c, as well as the conditions on γ and η_0 are quite strong, and does not truly capture the strength of Δ -SGD. Moreover, due to non-optimal implementation, Δ -SGD takes about $1.3\times$ more wall-clock time compared to SGD, which can be improved with more efficient implementation.

References

- [1] Agarwal, N., A. T. Suresh, F. X. X. Yu, S. Kumar, and B. McMahan (2018). cpSGD: Communication-efficient and differentially-private distributed SGD. *Advances in Neural Information Processing Systems* 31.
- [2] Armijo, L. (1966). Minimization of functions having lipschitz continuous first partial derivatives. *Pacific Journal of mathematics* 16(1), 1–3.
- [3] Assran, M., A. Aytekin, H. R. Feyzmahdavian, M. Johansson, and M. G. Rabbat (2020). Advances in asynchronous parallel and distributed optimization. *Proceedings of the IEEE* 108(11), 2013–2031.
- [4] Assran, M. and M. Rabbat (2020). On the convergence of nesterov’s accelerated gradient method in stochastic settings. *arXiv preprint arXiv:2002.12414*.
- [5] Bernstein, J., C. Mingard, K. Huang, N. Azizan, and Y. Yue (2023). Automatic gradient descent: Deep learning without hyperparameters. *arXiv preprint arXiv:2304.05187*.
- [6] Bottou, L., F. E. Curtis, and J. Nocedal (2018). Optimization methods for large-scale machine learning. *SIAM review* 60(2), 223–311.
- [7] Boyd, S., S. P. Boyd, and L. Vandenberghe (2004). *Convex optimization*. Cambridge university press.
- [8] Cauchy, A. et al. (1847). Méthode générale pour la résolution des systemes d’équations simultanées. *Comp. Rend. Sci. Paris* 25(1847), 536–538.
- [9] Cevher, V. and B. C. Vü (2019). On the linear convergence of the stochastic gradient method with constant step-size. *Optimization Letters* 13(5), 1177–1187.
- [10] Defazio, A. and K. Mishchenko (2023). Learning-rate-free learning by d-adaptation. *arXiv preprint arXiv:2301.07733*.
- [11] Defazio, A., B. Zhou, and L. Xiao (2022). Grad-gradograd? a non-monotone adaptive stochastic gradient method. *arXiv preprint arXiv:2206.06900*.
- [12] Drori, Y. and M. Teboulle (2014). Performance of first-order methods for smooth convex minimization: a novel approach. *Mathematical Programming* 145(1-2), 451–482.
- [13] Duchi, J., E. Hazan, and Y. Singer (2011). Adaptive subgradient methods for online learning and stochastic optimization. *Journal of machine learning research* 12(7).
- [14] Ghadimi, S. and G. Lan (2013). Stochastic first-and zeroth-order methods for nonconvex stochastic programming. *SIAM Journal on Optimization* 23(4), 2341–2368.
- [15] Gower, R. M., P. Richtárik, and F. Bach (2021). Stochastic quasi-gradient methods: Variance reduction via jacobian sketching. *Mathematical Programming* 188, 135–192.
- [16] Gower, R. M., M. Schmidt, F. Bach, and P. Richtárik (2020). Variance-reduced methods for machine learning. *Proceedings of the IEEE* 108(11), 1968–1983.
- [17] Hazan, E. and S. Kakade (2019). Revisiting the polyak step size. *arXiv preprint arXiv:1905.00313*.
- [18] He, K., X. Zhang, S. Ren, and J. Sun (2016). Deep residual learning for image recognition. In *Proceedings of the IEEE conference on computer vision and pattern recognition*, pp. 770–778.
- [19] Hsu, T.-M. H., H. Qi, and M. Brown (2019). Measuring the effects of non-identical data distribution for federated visual classification. *arXiv preprint arXiv:1909.06335*.
- [20] Johnson, R. and T. Zhang (2013). Accelerating stochastic gradient descent using predictive variance reduction. *Advances in neural information processing systems* 26.

- [21] Karimireddy, S. P., M. Jaggi, S. Kale, M. Mohri, S. J. Reddi, S. U. Stich, and A. T. Suresh (2020). Mime: Mimicking centralized stochastic algorithms in federated learning. *arXiv preprint arXiv:2008.03606*.
- [22] Khaled, A., K. Mishchenko, and P. Richtárik (2020). Tighter theory for local sgd on identical and heterogeneous data. In *International Conference on Artificial Intelligence and Statistics*, pp. 4519–4529. PMLR.
- [23] Kim, J. L., P. Toulis, and A. Kyrillidis (2022). Convergence and stability of the stochastic proximal point algorithm with momentum. In *Learning for Dynamics and Control Conference*, pp. 1034–1047. PMLR.
- [24] Kingma, D. P. and J. Ba (2014). Adam: A method for stochastic optimization. *arXiv preprint arXiv:1412.6980*.
- [25] Koloskova, A., N. Loizou, S. Boreiri, M. Jaggi, and S. Stich (2020). A unified theory of decentralized sgd with changing topology and local updates. In *International Conference on Machine Learning*, pp. 5381–5393. PMLR.
- [26] Krizhevsky, A., G. Hinton, et al. (2009). Learning multiple layers of features from tiny images.
- [27] Lan, G., S. Lee, and Y. Zhou (2020). Communication-efficient algorithms for decentralized and stochastic optimization. *Mathematical Programming* 180(1-2), 237–284.
- [28] Latafat, P., A. Themelis, L. Stella, and P. Patrinos (2023). Adaptive proximal algorithms for convex optimization under local lipschitz continuity of the gradient. *arXiv preprint arXiv:2301.04431*.
- [29] Levy, K. Y., A. Yurtsever, and V. Cevher (2018). Online adaptive methods, universality and acceleration. *Advances in neural information processing systems* 31.
- [30] Li, Q., B. He, and D. Song (2021). Model-contrastive federated learning. In *Proceedings of the IEEE/CVF Conference on Computer Vision and Pattern Recognition*, pp. 10713–10722.
- [31] Li, T., A. K. Sahu, M. Zaheer, M. Sanjabi, A. Talwalkar, and V. Smith (2020). Federated optimization in heterogeneous networks. *Proceedings of Machine learning and systems* 2, 429–450.
- [32] Liang, X., S. Shen, J. Liu, Z. Pan, E. Chen, and Y. Cheng (2019). Variance reduced local sgd with lower communication complexity. *arXiv preprint arXiv:1912.12844*.
- [33] Loizou, N., S. Vaswani, I. H. Laradji, and S. Lacoste-Julien (2021). Stochastic polyak step-size for sgd: An adaptive learning rate for fast convergence. In *International Conference on Artificial Intelligence and Statistics*, pp. 1306–1314. PMLR.
- [34] Malitsky, Y. and K. Mishchenko (2020). Adaptive gradient descent without descent. In *Proceedings of the 37th International Conference on Machine Learning*, Volume 119 of *Proceedings of Machine Learning Research*, pp. 6702–6712. PMLR.
- [35] McMahan, B., E. Moore, D. Ramage, S. Hampson, and B. A. y Arcas (2017). Communication-efficient learning of deep networks from decentralized data. In *Artificial intelligence and statistics*, pp. 1273–1282. PMLR.
- [36] Moulines, E. and F. Bach (2011). Non-asymptotic analysis of stochastic approximation algorithms for machine learning. *Advances in neural information processing systems* 24.
- [37] Nesterov, Y. (2003). *Introductory lectures on convex optimization: A basic course*, Volume 87. Springer Science & Business Media.
- [38] Nesterov, Y. (2015). Universal gradient methods for convex optimization problems. *Mathematical Programming* 152(1-2), 381–404.
- [39] Nguyen, J., K. Malik, H. Zhan, A. Yousefpour, M. Rabbat, M. Malek, and D. Huba (2022). Federated learning with buffered asynchronous aggregation. In *International Conference on Artificial Intelligence and Statistics*, pp. 3581–3607. PMLR.

- [40] Orabona, F. and D. Pál (2016). Coin betting and parameter-free online learning. *Advances in Neural Information Processing Systems* 29.
- [41] Paquette, C. and K. Scheinberg (2020). A stochastic line search method with expected complexity analysis. *SIAM Journal on Optimization* 30(1), 349–376.
- [42] Paszke, A., S. Gross, F. Massa, A. Lerer, J. Bradbury, G. Chanan, T. Killeen, Z. Lin, N. Gimelshein, L. Antiga, A. Desmaison, A. Kopf, E. Yang, Z. DeVito, M. Raison, A. Tejani, S. Chilamkurthy, B. Steiner, L. Fang, J. Bai, and S. Chintala (2019). Pytorch: An imperative style, high-performance deep learning library. In *Advances in Neural Information Processing Systems* 32, pp. 8024–8035. Curran Associates, Inc.
- [43] Polyak, B. T. (1963). Gradient methods for the minimisation of functionals. *USSR Computational Mathematics and Mathematical Physics* 3(4), 864–878.
- [44] Polyak, B. T. (1969). Minimization of nonsmooth functionals. *Zhurnal Vychislitel’noi Matematiki i Matematicheskoi Fiziki* 9(3), 509–521.
- [45] Praneeth Karimireddy, S., S. Kale, M. Mohri, S. J. Reddi, S. U. Stich, and A. Theertha Suresh (2019). Scaffold: Stochastic controlled averaging for federated learning. *arXiv e-prints*, arXiv–1910.
- [46] Qu, G. and N. Li (2019). Accelerated distributed nesterov gradient descent. *IEEE Transactions on Automatic Control* 65(6), 2566–2581.
- [47] Reddi, S. J., Z. Charles, M. Zaheer, Z. Garrett, K. Rush, J. Konečný, S. Kumar, and H. B. McMahan (2021). Adaptive federated optimization. In *International Conference on Learning Representations*.
- [48] Scaman, K., F. Bach, S. Bubeck, Y. T. Lee, and L. Massoulié (2017). Optimal algorithms for smooth and strongly convex distributed optimization in networks. In *international conference on machine learning*, pp. 3027–3036. PMLR.
- [49] Schmidt, M. and N. L. Roux (2013). Fast convergence of stochastic gradient descent under a strong growth condition. *arXiv preprint arXiv:1308.6370*.
- [50] Stich, S. U. (2018). Local sgd converges fast and communicates little. *arXiv preprint arXiv:1805.09767*.
- [51] Toghiani, M. T., S. Lee, and C. A. Uribe (2022). PersA-FL: Personalized Asynchronous Federated Learning. *arXiv preprint arXiv:2210.01176*.
- [52] Toulis, P. and E. M. Airoldi (2017). Asymptotic and finite-sample properties of estimators based on stochastic gradients.
- [53] Uribe, C. A., S. Lee, A. Gasnikov, and A. Nedić (2020). A dual approach for optimal algorithms in distributed optimization over networks. In *2020 Information Theory and Applications Workshop (ITA)*, pp. 1–37. IEEE.
- [54] Vaswani, S., F. Bach, and M. Schmidt (2019). Fast and faster convergence of sgd for over-parameterized models and an accelerated perceptron. In *The 22nd international conference on artificial intelligence and statistics*, pp. 1195–1204. PMLR.
- [55] Vaswani, S., A. Mishkin, I. Laradji, M. Schmidt, G. Gidel, and S. Lacoste-Julien (2019). Painless stochastic gradient: Interpolation, line-search, and convergence rates. *Advances in neural information processing systems* 32.
- [56] Wah, C., S. Branson, P. Welinder, P. Perona, and S. Belongie (2011). The caltech-ucsd birds-200-2011 dataset.
- [57] Wang, J., Z. Xu, Z. Garrett, Z. Charles, L. Liu, and G. Joshi (2021). Local adaptivity in federated learning: Convergence and consistency. *arXiv preprint arXiv:2106.02305*.
- [58] Ward, R., X. Wu, and L. Bottou (2020). Adagrad stepsizes: Sharp convergence over nonconvex landscapes. *The Journal of Machine Learning Research* 21(1), 9047–9076.

- [59] Xie, C., O. Koyejo, I. Gupta, and H. Lin (2019). Local adaalter: Communication-efficient stochastic gradient descent with adaptive learning rates. *arXiv preprint arXiv:1911.09030*.
- [60] Xie, C., S. Koyejo, and I. Gupta (2019). Asynchronous federated optimization. *arXiv preprint arXiv:1903.03934*.
- [61] Yousefpour, A., S. Guo, A. Shenoy, S. Ghosh, P. Stock, K. Maeng, S.-W. Krüger, M. Rabbat, C.-J. Wu, and I. Mironov (2023). Green federated learning. *arXiv preprint arXiv:2303.14604*.
- [62] Yuan, K., Q. Ling, and W. Yin (2016). On the convergence of decentralized gradient descent. *SIAM Journal on Optimization* 26(3), 1835–1854.
- [63] Zaheer, M., S. Reddi, D. Sachan, S. Kale, and S. Kumar (2018). Adaptive methods for nonconvex optimization. *Advances in neural information processing systems* 31.

Supplementary Materials for “Adaptive Federated Learning with Auto-Tuned Clients”

In this appendix, we provide all missing proofs that were not present in the main text, as well as additional plots and experiments. The appendix is organized as follows.

- In Appendix A, we provide all the missing proofs. In particular:
 - In Section A.1, we provide the proof of Algorithm 1, under Assumption 1.
 - In Section A.2, we provide the proof of Algorithm, 1, with some additional assumptions, including that f_i is convex for all $i \in [m]$.
 - In Section A.3, we provide a simple proof in the centralized nonconvex setting, which was an open question posed in [34].
- In Appendix B, we provide additional experiments, as well as miscellaneous plots that were missing in the main text due to the space constraints. Specifically:
 - In Section B.1, we provide some perspectives on the ease of tuning of Δ -SGD in Algorithm 1.
 - In Section B.2, we provide illustration of the different level of heterogeneity induced by the Dirichlet concentration parameter α .
 - In Section B.3, we provide some perspectives on how Δ -SGD performs using different number of local iterations.
 - In Section B.4, we provide additional experimental results where each client has different number of samples as local dataset.

A Missing Proofs

We first introduce the following two inequalities which will be used in the following proofs.

$$\langle x_i, x_j \rangle \leq \frac{1}{2} \|x_i\|^2 + \frac{1}{2} \|x_j\|^2, \quad \text{and} \quad (7)$$

$$\left\| \sum_{i=1}^m x_i \right\|^2 \leq m \sum_{i=1}^m \|x_i\|^2, \quad (8)$$

for any set of m vectors $\{x_i\}_{i=1}^m$ such that $x_i \in \mathbb{R}^d$.

We also provide the following lemma, which establishes \tilde{L} -smoothness based on local smoothness, *without assuming the global L -smoothness*.

Lemma 2. *For locally smooth function f_i , the following holds for the points that Algorithm 1 visits:*

$$f_i(x_t) \leq f_i(x_{t-1}) + \langle \nabla f_i(x_{t-1}), x_t - x_{t-1} \rangle + \frac{1}{4\eta_t^i} \|x_t - x_{t-1}\|^2. \quad (9)$$

Proof. By the definition of η_t^i , we have

$$\|\nabla f_i(x_t) - \nabla f_i(x_{t-1})\| \leq \frac{1}{2\eta_t^i} \|x_t - x_{t-1}\|$$

Thus, we have

$$\begin{aligned} \langle \nabla f_i(x_t) - \nabla f_i(x_{t-1}), x_t - x_{t-1} \rangle &\leq \|\nabla f_i(x_t) - \nabla f_i(x_{t-1})\| \cdot \|x_t - x_{t-1}\| \\ &\leq \frac{1}{2\eta_t^i} \|x_t - x_{t-1}\|^2. \end{aligned}$$

Let $g(k) = f_i(x_{t-1} + k(x_t - x_{t-1}))$. Then, we have

$$\begin{aligned} g'(k) &= \langle \nabla f_i(x_{t-1} + k(x_t - x_{t-1})), x_t - x_{t-1} \rangle \\ g'(k) - g'(0) &= \langle \nabla f_i(x_{t-1} + k(x_t - x_{t-1})) - \nabla f_i(x_{t-1}), \frac{k}{k}(x_t - x_{t-1}) \rangle \\ &\leq \frac{k}{2\eta_t^i} \|x_t - x_{t-1}\|^2. \end{aligned}$$

Using the Mean Value Theorem, we have

$$\begin{aligned} f_i(x_t) &= g(1) = g(0) + \int_0^1 g'(k) dk \\ &\leq g(0) + \int_0^1 [g'(0) + \frac{k}{2\eta_t^i} \|x_t - x_{t-1}\|] dk \\ &\leq g(0) + g'(0) + \frac{1}{4\eta_t^i} \|x_t - x_{t-1}\|^2 \\ &\leq f_i(x_{t-1}) + \langle \nabla f_i(x_{t-1}), x_t - x_{t-1} \rangle + \frac{1}{4\eta_t^i} \|x_t - x_{t-1}\|^2. \end{aligned}$$

□

We also establish the averaged version of local \tilde{L} -smoothness. First, we re-write the statement of Lemma 2 as follows:

$$\|\nabla f_i(x) - \nabla f_i(y)\|^2 \leq \tilde{L}_i \|x - y\|^2, \quad (10)$$

where \tilde{L}_i is $\max_t \left(\frac{1}{2\eta_t^i} \right)$ for all $x, y \in \text{conv}\{x_0, x_1, \dots\}$, and $\text{conv}\{\dots\}$ denotes the convex hull of the arguments [7]. Now, given (10),

Lemma 3. *The average of \tilde{L} -local smooth functions f_i are at least \tilde{L} -local smooth, where $\tilde{L} = \frac{1}{m} \sum_{i=1}^m \tilde{L}_i$.*

Proof. Starting from (10), we have:

$$\begin{aligned} \left\| \frac{1}{m} \sum_{i=1}^m \nabla f_i(x) - \frac{1}{m} \sum_{i=1}^m \nabla f_i(y) \right\| &= \left\| \frac{1}{m} \sum_{i=1}^m (\nabla f_i(x) - \nabla f_i(y)) \right\| \\ &\leq \frac{1}{m} \sum_{i=1}^m \|\nabla f_i(x) - \nabla f_i(y)\| \\ &\leq \frac{1}{m} \sum_{i=1}^m \tilde{L}_i \|x - y\| \\ &= \tilde{L} \|x - y\|. \end{aligned} \quad (11)$$

□

A.1 Proof of Algorithm 1 under Assumption 1

Proof. Based on Algorithm 1, we use the following notations throughout the proof:

$$\begin{aligned} x_{t,0}^i &= x_t, \\ x_{t,k}^i &= x_{t,k-1}^i - \eta_{t,k}^i \tilde{\nabla} f_i(x_{t,k-1}^i), \quad \forall k \in [K], \\ x_{t+1} &= \frac{1}{|\mathcal{S}_t|} \sum_{i \in \mathcal{S}_t} x_{t,k}^i, \end{aligned}$$

where we denoted with x_{t+1} as the server parameter at round $t + 1$, which is the average of the local parameters $x_{t,k}^i$ for all client $\forall i \in [m]$ after running k local iterations for $\forall k \in [K]$.

We start from the smoothness of $f(\cdot)$, which we emphasize again that is obtained via Lemma 3, i.e., as a byproduct of our analysis, and we do not assume that f_i 's are *globally* L -smooth. Also note that Lemma 3 holds for $\text{conv}\{x_0, x_1, \dots\}$, i.e., the average of the local parameters visited by Algorithm 1.

Proceeding, we have

$$f(x_{t+1}) \leq f(x_t) - \left\langle \nabla f(x_t), \frac{1}{|\mathcal{S}_t|} \sum_{i \in \mathcal{S}_t} \sum_{k=0}^{K-1} \eta_{t,k}^i \tilde{\nabla} f_i(x_{t,k}^i) \right\rangle + \frac{\tilde{L}}{2} \left\| \frac{1}{|\mathcal{S}_t|} \sum_{i \in \mathcal{S}_t} \sum_{k=0}^{K-1} \eta_{t,k}^i \tilde{\nabla} f_i(x_{t,k}^i) \right\|^2.$$

Taking expectation from the expression above, we get

$$\begin{aligned} & \mathbb{E}f(x_{t+1}) \\ & \leq f(x_t) - \mathbb{E} \left\langle \nabla f(x_t), \frac{1}{|\mathcal{S}_t|} \sum_{i \in \mathcal{S}_t} \sum_{k=0}^{K-1} \eta_{t,k}^i \tilde{\nabla} f_i(x_{t,k}^i) \right\rangle + \frac{\tilde{L}}{2} \mathbb{E} \left\| \frac{1}{|\mathcal{S}_t|} \sum_{i \in \mathcal{S}_t} \sum_{k=0}^{K-1} \eta_{t,k}^i \tilde{\nabla} f_i(x_{t,k}^i) \right\|^2 \end{aligned} \quad (12)$$

$$\leq f(x_t) - \mathbb{E} \left\langle \nabla f(x_t), \frac{1}{m} \sum_{i=1}^m \sum_{k=0}^{K-1} \eta_{t,k}^i \nabla f_i(x_{t,k}^i) \right\rangle + \frac{\tilde{L}}{2m} \sum_{i=1}^m \mathbb{E} \left\| \sum_{k=0}^{K-1} \eta_{t,k}^i \tilde{\nabla} f_i(x_{t,k}^i) \right\|^2 \quad (13)$$

$$\begin{aligned} & = f(x_t) - D_t \|\nabla f(x_t)\|^2 - D_t \mathbb{E} \left\langle \nabla f(x_t), \frac{1}{m} \sum_{i=1}^m \sum_{k=0}^{K-1} \frac{\eta_{t,k}^i}{D_t} \left(\nabla f_i(x_{t,k}^i) - \nabla f(x_t) \right) \right\rangle \\ & \quad + \frac{\tilde{L}}{2m} \sum_{i=1}^m \mathbb{E} \left\| \sum_{k=0}^{K-1} \eta_{t,k}^i \tilde{\nabla} f_i(x_{t,k}^i) \right\|^2, \end{aligned} \quad (14)$$

where in the equality, we added and subtracted $\frac{1}{m} \sum_{i=1}^m \sum_{k=0}^{K-1} \eta_{t,k}^i \nabla f(x_t)$ in the inner product term, and also replaced $D_t = \frac{1}{m} \sum_{i=1}^m \sum_{k=0}^{K-1} \eta_{t,k}^i$. Then, using (7) and (12)-(14), we have

$$\mathbb{E}f(x_{t+1}) \leq f(x_t) - D_t \|\nabla f(x_t)\|^2 + \frac{D_t}{2} \|\nabla f(x_t)\|^2 \quad (15)$$

$$\begin{aligned} & + \frac{D_t}{2} \mathbb{E} \left\| \frac{1}{m} \sum_{i=1}^m \sum_{k=0}^{K-1} \frac{\eta_{t,k}^i}{D_t} \left(\nabla f_i(x_{t,k}^i) - \nabla f(x_t) \right) \right\|^2 + \frac{\tilde{L}}{2m} \sum_{i=1}^m \mathbb{E} \left\| \sum_{k=0}^{K-1} \eta_{t,k}^i \tilde{\nabla} f_i(x_{t,k}^i) \right\|^2 \\ & = f(x_t) - \frac{D_t}{2} \|\nabla f(x_t)\|^2 + \frac{1}{2D_t} \mathbb{E} \left\| \frac{1}{m} \sum_{i=1}^m \sum_{k=0}^{K-1} \eta_{t,k}^i \left(\nabla f_i(x_{t,k}^i) - \nabla f(x_t) \right) \right\|^2 \\ & \quad + \frac{\tilde{L}}{2m} \sum_{i=1}^m \mathbb{E} \left\| \sum_{k=0}^{K-1} \eta_{t,k}^i \tilde{\nabla} f_i(x_{t,k}^i) \right\|^2 \end{aligned} \quad (16)$$

$$\begin{aligned} & = f(x_t) - \frac{D_t}{2} \|\nabla f(x_t)\|^2 \\ & \quad + \frac{1}{2D_t} \mathbb{E} \left\| \frac{1}{m} \sum_{i=1}^m \sum_{k=0}^{K-1} \eta_{t,k}^i \left(\nabla f_i(x_t) - \nabla f_i(x_{t,k}^i) + \nabla f_i(x_t) - \nabla f(x_t) \right) \right\|^2 \\ & \quad + \frac{\tilde{L}}{2m} \sum_{i=1}^m \mathbb{E} \left\| \sum_{k=0}^{K-1} \eta_{t,k}^i \left(\tilde{\nabla} f_i(x_{t,k}^i) - \nabla f_i(x_{t,k}^i) + \nabla f_i(x_{t,k}^i) - \nabla f_i(x_t) \right. \right. \\ & \quad \left. \left. + \nabla f_i(x_t) - \nabla f(x_t) + \nabla f(x_t) \right) \right\|^2 \end{aligned} \quad (17)$$

We now expand the terms in (17), and will bound each separately, as follows.

$$\begin{aligned} \mathbb{E}f(x_{t+1}) & \leq f(x_t) - \frac{D_t}{2} \|\nabla f(x_t)\|^2 \\ & \quad + \underbrace{\frac{1}{D_t} \mathbb{E} \left\| \frac{1}{m} \sum_{i=1}^m \sum_{k=0}^{K-1} \eta_{t,k}^i \left(\nabla f_i(x_t) - \nabla f_i(x_{t,k}^i) \right) \right\|^2}_{A_1} \end{aligned}$$

$$\begin{aligned}
& + \underbrace{\frac{1}{D_t} \mathbb{E} \left\| \frac{1}{m} \sum_{i=1}^m \sum_{k=0}^{K-1} \eta_{t,k}^i (\nabla f_i(x_t) - \nabla f(x_t)) \right\|^2}_{A_2} \\
& + \underbrace{\frac{2\tilde{L}}{m} \sum_{i=1}^m \mathbb{E} \left\| \sum_{k=0}^{K-1} \eta_{t,k}^i (\tilde{\nabla} f_i(x_{t,k}^i) - \nabla f_i(x_{t,k}^i)) \right\|^2}_{A_3} \\
& + \underbrace{\frac{2\tilde{L}}{m} \sum_{i=1}^m \mathbb{E} \left\| \sum_{k=0}^{K-1} \eta_{t,k}^i (\nabla f_i(x_{t,k}^i) - \nabla f_i(x_t)) \right\|^2}_{A_4} \\
& + \underbrace{\frac{2\tilde{L}}{m} \sum_{i=1}^m \mathbb{E} \left\| \sum_{k=0}^{K-1} \eta_{t,k}^i (\nabla f_i(x_t) - \nabla f(x_t)) \right\|^2}_{A_5} \\
& + \underbrace{\frac{2\tilde{L}}{m} \sum_{i=1}^m \mathbb{E} \left\| \sum_{k=0}^{K-1} \eta_{t,k}^i \nabla f(x_t) \right\|^2}_{A_6}. \tag{18}
\end{aligned}$$

Now, we provide an upper bound for each term in (18). Starting with A_1 , using (7), (8), and (11), we have

$$\begin{aligned}
A_1 & \leq \frac{K}{D_t m} \sum_{i=1}^m \sum_{k=0}^{K-1} (\eta_{t,k}^i)^2 \mathbb{E} \left\| \nabla f_i(x_t) - \nabla f_i(x_{t,k}^i) \right\|^2 \tag{19} \\
& \leq \frac{K\tilde{L}^2}{D_t m} \sum_{i=1}^m \sum_{k=0}^{K-1} (\eta_{t,k}^i)^2 \mathbb{E} \left\| x_t - x_{t,k}^i \right\|^2 \\
& = \frac{K\tilde{L}^2}{D_t m} \sum_{i=1}^m \sum_{k=0}^{K-1} (\eta_{t,k}^i)^2 \mathbb{E} \left\| \sum_{\ell=0}^{k-1} \eta_{t,\ell}^i \tilde{\nabla} f_i(x_{t,\ell}^i) \right\|^2 \\
& = \frac{K\tilde{L}^2}{D_t m} \sum_{i=1}^m \sum_{k=0}^{K-1} (\eta_{t,k}^i)^2 \mathbb{E} \left\| \sum_{\ell=0}^{k-1} \eta_{t,\ell}^i (\tilde{\nabla} f_i(x_{t,\ell}^i) - \nabla f_i(x_{t,\ell}^i) + \nabla f_i(x_{t,\ell}^i)) \right\|^2 \\
& \leq \frac{2K\tilde{L}^2}{D_t m} \sum_{i=1}^m \sum_{k=0}^{K-1} (\eta_{t,k}^i)^2 \left[\mathbb{E} \left\| \sum_{\ell=0}^{k-1} \eta_{t,\ell}^i (\tilde{\nabla} f_i(x_{t,\ell}^i) - \nabla f_i(x_{t,\ell}^i)) \right\|^2 + \mathbb{E} \left\| \sum_{\ell=0}^{k-1} \eta_{t,\ell}^i \nabla f_i(x_{t,\ell}^i) \right\|^2 \right] \\
& \leq \frac{2K\tilde{L}^2}{D_t m} \sum_{i=1}^m \sum_{k=0}^{K-1} k (\eta_{t,k}^i)^2 \sum_{\ell=0}^{k-1} (\eta_{t,\ell}^i)^2 \left[\mathbb{E} \left\| \tilde{\nabla} f_i(x_{t,\ell}^i) - \nabla f_i(x_{t,\ell}^i) \right\|^2 + \mathbb{E} \left\| \nabla f_i(x_{t,\ell}^i) \right\|^2 \right] \\
& \leq \frac{2K\tilde{L}^2}{D_t m} \sum_{i=1}^m \sum_{k=0}^{K-1} k (\eta_{t,k}^i)^2 \sum_{\ell=0}^{k-1} (\eta_{t,\ell}^i)^2 \left(\frac{\sigma^2}{b} + G^2 \right) \\
& \leq \frac{2K^2\tilde{L}^2 \left(\frac{\sigma^2}{b} + G^2 \right)}{D_t m} \sum_{i=1}^m \left(\sum_{k=0}^{K-1} (\eta_{t,k}^i)^2 \right)^2. \tag{20}
\end{aligned}$$

For A_2 , using (7) and (8), we have:

$$\begin{aligned}
A_2 & \leq \frac{K}{D_t m} \sum_{i=1}^m \sum_{k=0}^{K-1} (\eta_{t,k}^i)^2 \mathbb{E} \left\| \nabla f_i(x_t) - \nabla f(x_t) \right\|^2 \\
& \leq \frac{K\rho}{D_t m} \left\| \nabla f(x_t) \right\|^2 \sum_{i=1}^m \sum_{k=0}^{K-1} (\eta_{t,k}^i)^2. \tag{21}
\end{aligned}$$

For A_3 , using (7), (8), and (11), we have:

$$\begin{aligned} A_3 &\leq \frac{2K\tilde{L}}{m} \sum_{i=1}^m \sum_{k=0}^{K-1} (\eta_{t,k}^i)^2 \mathbb{E} \left\| \tilde{\nabla} f_i(x_{t,k}^i) - \nabla f_i(x_{t,k}^i) \right\|^2 \\ &\leq \frac{2K\tilde{L}\sigma^2}{mb} \sum_{i=1}^m \sum_{k=0}^{K-1} (\eta_{t,k}^i)^2. \end{aligned} \quad (22)$$

For A_4 , using (7), (8), and (11), we have:

$$\begin{aligned} A_4 &\leq \frac{2K\tilde{L}}{m} \sum_{i=1}^m \sum_{k=0}^{K-1} (\eta_{t,k}^i)^2 \mathbb{E} \left\| \nabla f_i(x_t) - \nabla f_i(x_{t,k}^i) \right\|^2 \\ &\leq \frac{2K\tilde{L}^3}{m} \sum_{i=1}^m \sum_{k=0}^{K-1} (\eta_{t,k}^i)^2 \mathbb{E} \left\| x_t - x_{t,k}^i \right\|^2 \\ &= \frac{2K\tilde{L}^3}{m} \sum_{i=1}^m \sum_{k=0}^{K-1} (\eta_{t,k}^i)^2 \mathbb{E} \left\| \sum_{\ell=0}^{k-1} \eta_{t,\ell}^i \tilde{\nabla} f_i(x_{t,\ell}^i) \right\|^2 \\ &= \frac{2K\tilde{L}^3}{m} \sum_{i=1}^m \sum_{k=0}^{K-1} (\eta_{t,k}^i)^2 \mathbb{E} \left\| \sum_{\ell=0}^{k-1} \eta_{t,\ell}^i \left(\tilde{\nabla} f_i(x_{t,\ell}^i) - \nabla f_i(x_{t,\ell}^i) + \nabla f_i(x_{t,\ell}^i) \right) \right\|^2 \\ &\leq \frac{4K\tilde{L}^3}{m} \sum_{i=1}^m \sum_{k=0}^{K-1} (\eta_{t,k}^i)^2 \left[\mathbb{E} \left\| \sum_{\ell=0}^{k-1} \eta_{t,\ell}^i \left(\tilde{\nabla} f_i(x_{t,\ell}^i) - \nabla f_i(x_{t,\ell}^i) \right) \right\|^2 + \mathbb{E} \left\| \sum_{\ell=0}^{k-1} \eta_{t,\ell}^i \nabla f_i(x_{t,\ell}^i) \right\|^2 \right] \\ &\leq \frac{4K\tilde{L}^3}{m} \sum_{i=1}^m \sum_{k=0}^{K-1} k (\eta_{t,k}^i)^2 \sum_{\ell=0}^{k-1} (\eta_{t,\ell}^i)^2 \left[\mathbb{E} \left\| \tilde{\nabla} f_i(x_{t,\ell}^i) - \nabla f_i(x_{t,\ell}^i) \right\|^2 + \mathbb{E} \left\| \nabla f_i(x_{t,\ell}^i) \right\|^2 \right] \\ &\leq \frac{4K\tilde{L}^3}{m} \sum_{i=1}^m \sum_{k=0}^{K-1} k (\eta_{t,k}^i)^2 \sum_{\ell=0}^{k-1} (\eta_{t,\ell}^i)^2 \left(\frac{\sigma^2}{b} + G^2 \right) \\ &\leq \frac{4K^2\tilde{L}^3 \left(\frac{\sigma^2}{b} + G^2 \right)}{m} \sum_{i=1}^m \left(\sum_{k=0}^{K-1} (\eta_{t,k}^i)^2 \right)^2. \end{aligned} \quad (24)$$

For A_5 , using (7), (8), and (11), we have:

$$\begin{aligned} A_5 &\leq \frac{2K\tilde{L}}{m} \sum_{i=1}^m \sum_{k=0}^{K-1} (\eta_{t,k}^i)^2 \mathbb{E} \left\| \nabla f_i(x_t) - \nabla f(x_t) \right\|^2 \\ &\leq \frac{2K\tilde{L}\rho}{m} \left\| \nabla f(x_t) \right\|^2 \sum_{i=1}^m \sum_{k=0}^{K-1} (\eta_{t,k}^i)^2. \end{aligned} \quad (25)$$

For A_6 , using (7), (8), and (11), we have:

$$A_6 \leq \frac{2K\tilde{L}}{m} \left\| \nabla f(x_t) \right\|^2 \sum_{i=1}^m \sum_{k=0}^{K-1} (\eta_{t,k}^i)^2. \quad (26)$$

Putting all bounds together. Now, by putting (19)–(26) back into (18) and rearranging the terms, we obtain the following inequality:

$$\begin{aligned} &\left(\frac{D_t}{2} - \frac{K\rho}{D_t m} \sum_{i=1}^m \sum_{k=0}^{K-1} (\eta_{t,k}^i)^2 - \frac{2K\tilde{L}(1+\rho)}{m} \sum_{i=1}^m \sum_{k=0}^{K-1} (\eta_{t,k}^i)^2 \right) \left\| \nabla f(x_t) \right\|^2 \\ &\leq f(x_t) - f(x_{t+1}) + \frac{2K^2\tilde{L}^2 \left(\frac{\sigma^2}{b} + G^2 \right)}{D_t m} \sum_{i=1}^m \left(\sum_{k=0}^{K-1} (\eta_{t,k}^i)^2 \right)^2 \end{aligned}$$

$$+ \frac{2K\tilde{L}\sigma^2}{mb} \sum_{i=1}^m \sum_{k=0}^{K-1} (\eta_{t,k}^i)^2 + \frac{4K^2\tilde{L}^3 \left(\frac{\sigma^2}{b} + G^2 \right)}{m} \sum_{i=1}^m \left(\sum_{k=0}^{K-1} (\eta_{t,k}^i)^2 \right)^2. \quad (27)$$

Now, it remains to notice that, by definition, $\eta_{t,k}^i = \mathcal{O}(\gamma)$, for all $i \in [m], k \in \{0, 1, \dots, K-1\}$, and $t \geq 0$. Therefore, $D_t = \mathcal{O}(\gamma K)$. Thus, by dividing the above inequality by $\frac{D_t}{2}$, we have:

$$\begin{aligned} & \left(1 - \underbrace{\frac{2K\rho}{D_t^2 m} \sum_{i=1}^m \sum_{k=0}^{K-1} (\eta_{t,k}^i)^2}_{\mathcal{O}(1)} - \underbrace{\frac{4K\tilde{L}(1+\rho)}{D_t m} \sum_{i=1}^m \sum_{k=0}^{K-1} (\eta_{t,k}^i)^2}_{\mathcal{O}(\gamma K)} \right) \|\nabla f(x_t)\|^2 \\ & \leq \underbrace{\frac{2(f(x_t) - f(x_{t+1}))}{D_t}}_{\mathcal{O}\left(\frac{1}{\gamma K}\right)} + \underbrace{\frac{4K\tilde{L}\sigma^2}{D_t mb} \sum_{i=1}^m \sum_{k=0}^{K-1} (\eta_{t,k}^i)^2}_{\mathcal{O}(\gamma K)} \\ & \quad + \underbrace{\frac{4K^2\tilde{L}^2 \left(\frac{\sigma^2}{b} + G^2 \right)}{D_t^2 m} \sum_{i=1}^m \left(\sum_{k=0}^{K-1} (\eta_{t,k}^i)^2 \right)^2}_{\mathcal{O}(\gamma^2 K^2)} \\ & \quad + \underbrace{\frac{8K^2\tilde{L}^3 \left(\frac{\sigma^2}{b} + G^2 \right)}{D_t m} \sum_{i=1}^m \left(\sum_{k=0}^{K-1} (\eta_{t,k}^i)^2 \right)^2}_{\mathcal{O}(\gamma^3 K^3)}, \end{aligned} \quad (28)$$

for $\rho = \mathcal{O}(1)$. For the simplicity of exposition, assuming $\rho \leq \frac{1}{4}$ and $T \geq (5/\rho)^2 = 400$, we obtain the below by averaging (28) for $t = 0, 1, \dots, T-1$:

$$\begin{aligned} \frac{1}{T} \sum_{t=0}^{T-1} \|\nabla f(x_t)\|^2 & \leq \mathcal{O}\left(\frac{f(x_0) - f^*}{\gamma KT}\right) + \mathcal{O}\left(\frac{\gamma K \sigma^2}{b}\right) + \mathcal{O}\left(\tilde{L}^2 \left(\frac{\sigma^2}{b} + G^2\right) \gamma^2 K^2\right) \\ & \quad + \mathcal{O}\left(\tilde{L}^3 \left(\frac{\sigma^2}{b} + G^2\right) \gamma^3 K^3\right). \end{aligned} \quad (29)$$

Finally, by choosing $\gamma = \mathcal{O}\left(\frac{1}{K\sqrt{T}}\right)$, and defining $\Psi_1 = \max\left\{\frac{\sigma^2}{b}, f(x_0) - f(x^*)\right\}$ and $\Psi_2 = \left(\frac{\sigma^2}{b} + G^2\right)$ with $b = |\mathcal{B}|$ being the batch size, we arrive at the statement in Theorem 1, i.e.,

$$\frac{1}{T} \sum_{t=0}^{T-1} \mathbb{E} \|\nabla f(x_t)\|^2 \leq \mathcal{O}\left(\frac{\Psi_1}{\sqrt{T}}\right) + \mathcal{O}\left(\frac{\tilde{L}^2 \Psi_2}{T}\right) + \mathcal{O}\left(\frac{\tilde{L}^3 \Psi_2}{\sqrt{T^3}}\right).$$

□

A.2 Proof of Algorithm 1 for convex case

Here, we provide an extension of the proof of [34, Theorem 1] for distributed version. Note that the proof we provide here is not exactly the same version of Δ -SGD presented in Algorithm 1; in particular, we assume no local iterations, i.e., $k = 1$ for all $i \in [m]$, and every client participate, i.e., $p = 1$.

We start with the extension of [34, Lemma 1], which constructs a Lyapunov function for the distributed objective in (1).

Lemma 4. *Let $f_i : \mathbb{R}^d \rightarrow \mathbb{R}$ be convex and twice differentiable. Then, the sequence $\{x_t\}$ generated by Algorithm 1, assuming $k = 1$ and $p = 1$, satisfy the following:*

$$\|x_{t+1} - x^*\|^2 + \frac{1}{2m} \sum_{i=1}^m \|x_{t+1}^i - x_t^i\|^2 + \frac{2}{m} \sum_{i=1}^m \left[\eta_t^i (1 + \theta_t^i) (f_i(x_t^i) - f_i(x^*)) \right]$$

$$\leq \|x_t - x^*\|^2 + \frac{1}{2m} \sum_{i=1}^m \|x_t^i - x_{t-1}^i\|^2 + \frac{2}{m} \sum_{i=1}^m \left[\eta_t^i \theta_t^i (f_i(x_{t-1}^i) - f_i(x^*)) \right]. \quad (30)$$

The above lemma, which we prove below, constructs a contracting Lyapunov function, which can be seen from the second condition on the step size η_t^i :

$$\eta_{t+1}^i \leq \sqrt{1 + \theta_t^i \eta_t^i} \implies \eta_{t+1}^i \theta_{t+1}^i \leq (1 + \theta_t^i) \eta_t^i.$$

Proof. We denote $x_t = \frac{1}{m} \sum_{i=1}^m x_t^i$.

$$\|x_{t+1} - x^*\|^2 = \left\| x_t - \frac{1}{m} \sum_{i=1}^m \eta_t^i \nabla f_i(x_t^i) - x^* \right\|^2 \quad (31)$$

$$= \|x_t - x^*\|^2 + \left\| \frac{1}{m} \sum_{i=1}^m \eta_t^i \nabla f_i(x_t^i) \right\|^2 - 2 \left\langle x_t - x^*, \frac{1}{m} \sum_{i=1}^m \eta_t^i \nabla f_i(x_t^i) \right\rangle \quad (32)$$

We will first bound the second term in (32). Using $\left\| \sum_{i=1}^m a_i \right\|^2 \leq m \cdot \sum_{i=1}^m \|a_i\|^2$, we have

$$\left\| \frac{1}{m} \sum_{i=1}^m \eta_t^i \nabla f_i(x_t^i) \right\|^2 = \left\| \frac{1}{m} \sum_{i=1}^m (x_t^i - x_{t+1}^i) \right\|^2 \leq \frac{1}{m} \sum_{i=1}^m \|x_t^i - x_{t+1}^i\|^2. \quad (33)$$

To bound $\|x_t^i - x_{t+1}^i\|^2$, observe that

$$\begin{aligned} \|x_t^i - x_{t+1}^i\|^2 &= 2\|x_t^i - x_{t+1}^i\|^2 - \|x_t^i - x_{t+1}^i\|^2 \\ &= 2\langle -\eta_t^i \nabla f_i(x_t^i), x_t^i - x_{t+1}^i \rangle - \|x_t^i - x_{t+1}^i\|^2 \\ &= 2\eta_t^i \langle \nabla f_i(x_t^i) - \nabla f_i(x_{t-1}^i), x_{t+1}^i - x_t^i \rangle - \|x_t^i - x_{t+1}^i\|^2 \\ &\quad + 2\eta_t^i \langle \nabla f_i(x_{t-1}^i), x_{t+1}^i - x_t^i \rangle \end{aligned} \quad (34)$$

For the first term in (34), using Cauchy-Schwarz and Young's inequalities as well as

$$\eta_t^i \leq \frac{\|x_t^i - x_{t-1}^i\|}{2\|\nabla f_i(x_t^i) - \nabla f_i(x_{t-1}^i)\|}, \text{ we have:}$$

$$\begin{aligned} 2\eta_t^i \langle \nabla f_i(x_t^i) - \nabla f_i(x_{t-1}^i), x_{t+1}^i - x_t^i \rangle &\leq 2\eta_t^i \|\nabla f_i(x_t^i) - \nabla f_i(x_{t-1}^i)\| \cdot \|x_{t+1}^i - x_t^i\| \\ &\leq \|x_t^i - x_{t-1}^i\| \cdot \|x_{t+1}^i - x_t^i\| \\ &\leq \frac{1}{2} \|x_t^i - x_{t-1}^i\|^2 + \frac{1}{2} \|x_{t+1}^i - x_t^i\|^2. \end{aligned}$$

For the third term in (34), by convexity of $f_i(x)$, we have

$$\begin{aligned} 2\eta_t^i \langle \nabla f_i(x_{t-1}^i), x_{t+1}^i - x_t^i \rangle &= 2\frac{\eta_t^i}{\eta_{t-1}^i} \langle x_{t-1}^i - x_t^i, x_{t+1}^i - x_t^i \rangle \\ &= 2\theta_t^i \eta_t^i \langle x_{t-1}^i - x_t^i, \nabla f_i(x_t^i) \rangle \\ &\leq 2\theta_t^i \eta_t^i [f_i(x_{t-1}^i) - f_i(x_t^i)]. \end{aligned}$$

Together, we have

$$\frac{1}{m} \sum_{i=1}^m \|x_t^i - x_{t+1}^i\|^2 \leq \frac{1}{m} \sum_{i=1}^m \left\{ \frac{1}{2} \|x_t^i - x_{t-1}^i\|^2 - \frac{1}{2} \|x_{t+1}^i - x_t^i\|^2 + 2\theta_t^i \eta_t^i [f_i(x_{t-1}^i) - f_i(x_t^i)] \right\}. \quad (35)$$

Now to bound the last term in (32), we have

$$\begin{aligned} -2 \left\langle x_t - x^*, \frac{1}{m} \sum_{i=1}^m \eta_t^i \nabla f_i(x_t^i) \right\rangle &= \frac{2}{m} \eta_t^i \sum_{i=1}^m \langle x^* - x_t^i, \nabla f_i(x_t^i) \rangle \\ &\leq \frac{2}{m} \sum_{i=1}^m \eta_t^i (f_i(x^*) - f_i(x_t^i)), \end{aligned} \quad (36)$$

where in the equality we used the fact that $x_t^i = x_t$, for $k = 1$.

Putting (35) and (36) back to (32), we have

$$\begin{aligned} \|x_{t+1} - x^*\|^2 &= \|x_t - x^*\|^2 + \left\| \frac{1}{m} \sum_{i=1}^m \eta_t^i \nabla f_i(x_t^i) \right\|^2 - 2 \left\langle x_t - x^*, \frac{1}{m} \sum_{i=1}^m \eta_t^i \nabla f_i(x_t^i) \right\rangle \\ &\leq \|x_t - x^*\|^2 + \frac{1}{m} \sum_{i=1}^m \left\{ \frac{1}{2} \|x_t^i - x_{t-1}^i\|^2 - \frac{1}{2} \|x_{t+1}^i - x_t^i\|^2 + 2\theta_t^i \eta_t^i [f_i(x_{t-1}^i) - f_i(x_t^i)] \right\} \\ &\quad - 2 \left\langle x_t - x^*, \frac{1}{m} \sum_{i=1}^m \eta_t^i \nabla f_i(x_t^i) \right\rangle + 2 \frac{1}{m} \sum_{i=1}^m \eta_t^i (f_i(x^*) - f_i(x_t^i)). \end{aligned} \quad (37)$$

Averaging (37) for $i = 1, \dots, m$, notice that the first term in (37) disappears, as $\hat{x}_t = \frac{1}{m} \sum_{i=1}^m x_i$.

$$\begin{aligned} \|x_{t+1} - x^*\|^2 &+ \frac{1}{m} \sum_{i=1}^m \left[2\eta_t^i (1 + \theta_t^i) (f_i(x_t^i) - f_i(x^*)) + \frac{1}{2} \|x_{t+1}^i - x_t^i\|^2 \right] \\ &\leq \|x_t - x^*\|^2 + \frac{1}{m} \sum_{i=1}^m \left[2\eta_t^i \theta_t^i (f_i(x_{t-1}^i) - f_i(x^*)) + \frac{1}{2} \|x_t^i - x_{t-1}^i\|^2 \right]. \end{aligned}$$

□

Theorem 5. Let $f_i : \mathbb{R}^d \rightarrow \mathbb{R}$ be convex and twice differentiable. Then, the sequence $\{x_i\}$ generated by Algorithm 1, assuming $k = 1$ and $p = 1$, satisfy the following:

$$\frac{1}{m} \sum_{i=1}^m (f_i(\tilde{x}_t^i) - f_i(x^*)) \leq \frac{2DL^2}{2Lt + 1}, \quad (38)$$

where

$$\begin{aligned} \tilde{x}_t^i &= \frac{\eta_t^i (1 + \theta_t^i) x_t^i + \sum_{k=1}^{t-1} \alpha_k^i x_k^i}{S_t^i}, \\ \alpha_k^i &= \eta_k^i (1 + \theta_k^i) - \eta_{k+1}^i \theta_{k+1}^i \\ S_t^i &= \eta_t^i (1 + \theta_t^i) + \sum_{k=1}^{t-1} \alpha_k^i = \sum_{k=1}^t \eta_k^i + \eta_1^i \theta_1^i. \end{aligned}$$

Further, if x^* is any minimum of $f_i(x)$ for all $i \in [m]$, (38) implies convergence for problem (1).

Proof. We start by telescoping (30). Then, we arrive at

$$\begin{aligned} \|x_{t+1} - x^*\|^2 &+ \frac{1}{2m} \sum_{i=1}^m \|x_{t+1}^i - x_t^i\|^2 + \frac{2}{m} \sum_{i=1}^m \left[\eta_t^i (1 + \theta_t^i) (f_i(x_t^i) - f_i(x^*)) \right. \\ &\quad \left. + \sum_{k=1}^{t-1} (\eta_k^i (1 + \theta_k^i) - \eta_{k+1}^i \theta_{k+1}^i) (f_i(x_k^i) - f_i(x^*)) \right] \quad (39) \\ &\leq \|x_1 - x^*\|^2 + \frac{1}{2m} \sum_{i=1}^m \|x_1^i - x_0^i\|^2 + \frac{2}{m} \sum_{i=1}^m \eta_1^i \theta_1^i (f_i(x_0^i) - f_i(x^*)) := D. \quad (40) \end{aligned}$$

Observe that (39) is of the form $\alpha_t^i [f_i(x_t^i) - f_i(x^*)] + \sum_{k=1}^{t-1} \alpha_k^i [f_i(x_k^i) - f_i(x^*)] = \sum_{k=1}^t \alpha_k^i [f_i(x_k^i) - f_i(x^*)]$. The sum of the coefficients equals:

$$\sum_{k=1}^t \alpha_k^i = \eta_t^i (1 + \theta_t^i) + \sum_{k=1}^{t-1} [\eta_k^i (1 + \theta_k^i) - \eta_{k+1}^i \theta_{k+1}^i] = \eta_1^i \theta_1^i + \sum_{k=1}^t \eta_k^i := S_t^i. \quad (41)$$

Therefore, by Jensen's inequality, we have

$$D \geq \|x_1 - x^*\|^2 + \frac{1}{2m} \sum_{i=1}^m \|x_1^i - x_0^i\|^2 + 2S_t^i(f_i(\tilde{x}_t^i) - f_i(x^*)) \geq 2S_t^i(f_i(\tilde{x}_t^i) - f_i(x^*)), \quad (42)$$

which implies $f_i(\tilde{x}_t^i) - f_i(x^*) \leq \frac{D^i}{2S_t^i}$, where

$$\begin{aligned} \tilde{x}_t^i &= \frac{\eta_t^i(1 + \theta_t^i)x_t^i + \sum_{k=1}^{t-1} \alpha_k^i x_k^i}{S_t^i}, \\ \alpha_k^i &= \eta_k^i(1 + \theta_k^i) - \eta_{k+1}^i \theta_{k+1}^i \\ S_t^i &= \eta_t^i(1 + \theta_t^i) + \sum_{k=1}^{t-1} \alpha_k^i = \sum_{k=1}^t \eta_k^i + \eta_1^i \theta_1^i. \end{aligned} \quad (43)$$

Now, notice that by definition of η_t^i , we have

$$\eta_t^i = \frac{\|x_t^i - x_{t-1}^i\|}{2\|\nabla f(x_t^i) - \nabla f(x_{t-1}^i)\|} \geq \frac{1}{2\tilde{L}_i} \geq \frac{1}{2L}, \quad \forall i \in [m].$$

where \tilde{L}_i is defined in (10), which by definition is smaller than or equal to the global smoothness L . Also, notice that $\eta_1^i \theta_1^i = \frac{(\eta_1^i)^2}{\eta_0^i} = (\eta_1^i)^2$, assuming for simplicity that $\eta_0^i = 1$. Thus, going back to (43), we have

$$\begin{aligned} S_t^i &= \sum_{k=1}^t \eta_k^i + \eta_1^i \theta_1^i \geq \sum_{k=1}^t \frac{1}{2\tilde{L}_i} + \frac{1}{4\tilde{L}_i^2} \\ &= \frac{t}{2\tilde{L}_i} + \frac{1}{4\tilde{L}_i^2} \geq \frac{t}{2L} + \frac{1}{4L^2}. \end{aligned}$$

Finally, we have

$$\begin{aligned} \frac{D}{2} &\geq \frac{1}{m} \sum_{i=1}^m S_t^i(f_i(\tilde{x}_t^i) - f_i(x^*)) \\ &\geq \frac{1}{m} \sum_{i=1}^m \left(\frac{t}{2L} + \frac{1}{4L^2} \right) (f_i(\tilde{x}_t^i) - f_i(x^*)), \end{aligned}$$

which implies

$$\frac{2DL^2}{2Lt + 1} \geq \frac{1}{m} \sum_{i=1}^m (f_i(\tilde{x}_t^i) - f_i(x^*)).$$

□

A.3 Proof of adaptive gradient descent in nonconvex case: centralized

For the centralized version, we use the original step size from [34] as in (4).

Theorem 6. *Running gradient descent with step size in (4) for nonconvex f , it holds that*

$$\frac{1}{T} \sum_{t=0}^{T-1} \|\nabla f(x_t)\|^2 \leq \frac{8\tilde{L}}{3T} [f(x_0) - f^*],$$

where \tilde{L} is the local-smoothness on the set $\mathcal{C} = \text{conv}\{x_0, x_1, \dots\}$:

$$\|\nabla f(x) - \nabla f(y)\| \leq \tilde{L}\|x - y\| \quad \forall x, y \in \mathcal{C}$$

Proof. Using Lemma 2, where with slight abuse of notation we interpret f_i as f and η_t^i as η_t , we have

$$\begin{aligned} f(x_{t+1}) &\leq f(x_t) + \langle \nabla f(x_t), x_{t+1} - x_t \rangle + \frac{1}{4\eta_t} \|x_{t+1} - x_t\|^2 \\ &= f(x_t) + \langle \nabla f(x_t), -\eta_t \nabla f(x_t) \rangle + \frac{1}{4\eta_t} \|x_{t+1} - x_t\|^2 \\ &= f(x_t) - \eta_t \|\nabla f(x_t)\|^2 + \frac{\eta_t}{4} \|\nabla f(x_t)\|^2 \\ &= f(x_t) - \frac{3\eta_t}{4} \|\nabla f(x_t)\|^2 \end{aligned}$$

Rearranging, we have

$$\|\nabla f(x_t)\|^2 \leq \frac{4}{3\eta_t} [f(x_t) - f^* + f^* - f(x_{t-1})]$$

Unfolding for T iterations and using telescoping, we get

$$\frac{1}{T} \sum_{t=0}^{T-1} \|\nabla f(x_t)\|^2 \leq \frac{4}{3T\eta_t} [f(x_0) - f^*] \leq \frac{8\tilde{L}}{3T} [f(x_0) - f^*]$$

as desired. \square

B Additional Experiments and Plots

B.1 Ease of tuning

In this subsection, we show the effect of using different parameter δ in the step size of Δ -SGD. As mentioned in Section 4, for Δ -SGD, we append δ in front of the second condition, and hence the step size becomes

$$\eta_{t,k}^i = \min \left\{ \frac{\gamma \|x_{t,k}^i - x_{t,k-1}^i\|}{2 \|\nabla f_i(x_{t,k}^i) - \nabla f_i(x_{t,k-1}^i)\|}, \sqrt{1 + \delta \theta_{t,k-1}^i} \eta_{t,k-1}^i \right\}.$$

The experimental results presented in Table 1 were obtained using a value of $\delta = 0.1$. For γ , we remind the readers that we did not change from the default value $\gamma = 2$ in the original implementation in https://github.com/ymalitsky/adaptive_GD/blob/master/pytorch/optimizer.py.

In Figure 4, we display the final accuracy achieved when using different values of δ from the set $\{0.01, 0.1, 1\}$. Interestingly, we observe that δ has very little impact on the final accuracy. This suggests that Δ -SGD is remarkably robust and does not require much tuning, while consistently achieving higher test accuracy compared to other methods in the majority of cases as shown in Table 1.

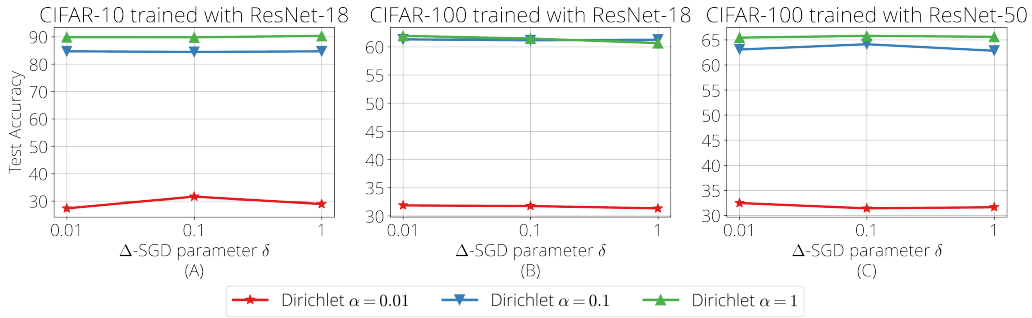


Figure 4: Effect of using different δ in the second condition of the step size of Δ -SGD.

B.2 Illustration of the degree of non-iidness

As mentioned in the main text, the level of "non-iidness" is controlled using latent Dirichlet allocation (LDA) applied to the labels. This approach is based on [19] and involves assigning each client a

multinomial distribution over the labels. This distribution determines the labels from which the client’s training examples are drawn. Specifically, the local training examples for each client are sampled from a categorical distribution over N classes, parameterized by a vector \mathbf{q} . The vector \mathbf{q} is drawn from a Dirichlet distribution with a concentration parameter α times a prior distribution vector \mathbf{p} over N classes.

To vary the level of "non-iidness," different values of α are considered: 0.01, 0.1, and 1. A larger α corresponds to settings that are closer to i.i.d. scenarios, while smaller values introduce more diversity and non-iidness among the clients, as visualized in Figure 5. As can be seen, for $\alpha = 1$, each client (each row on y -axis) have fairly diverse classes, similarly to the i.i.d. case; as we decrease α , the number of classes that each client has access to decreases. With $\alpha = 0.01$, there are many clients who only have access to a single or a couple classes.

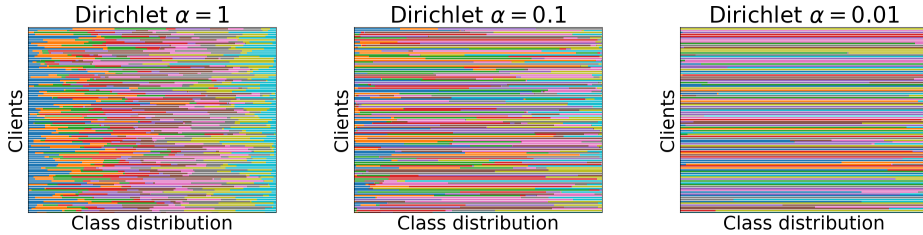


Figure 5: Illustration of the degree of heterogeneity induced by using different concentration parameter α for Dirichlet distribution, for CIFAR-10 dataset (10 colors) and 100 clients (100 rows on y -axis).

B.3 Effect of different number of local iterations

In this subsection, we show the effect of different number of local epochs performed per client, while fixing the experimental setup to be the classification of CIFAR-100 dataset, trained with a ResNet-50. We show for all three cases of the Dirichlet concentration parameter $\alpha \in \{0.01, 0.1, 1\}$. The result is shown in Figure 6.

As mentioned in the main text, instead of performing local iterations, we instead perform local epochs E , similarly to [47, 31]. All the results in Table 1 use $E = 1$, and in Figure 6, we show the results for $E \in \{1, 2, 3\}$. Note that in terms of E , the considered numbers might be small difference, but in terms of actual local gradient steps, they differ significantly.

As can be seen, using higher E leads to slightly faster convergence in all cases of α . However, the speed up seems marginal compared to the amount of extra computation time it requires (i.e., using $E = 2$ takes roughly twice more total wall-clock time than using $E = 1$). Put differently, Δ -SGD performs well with only using a single local epoch per client ($E = 1$), and still can achieve great performance.

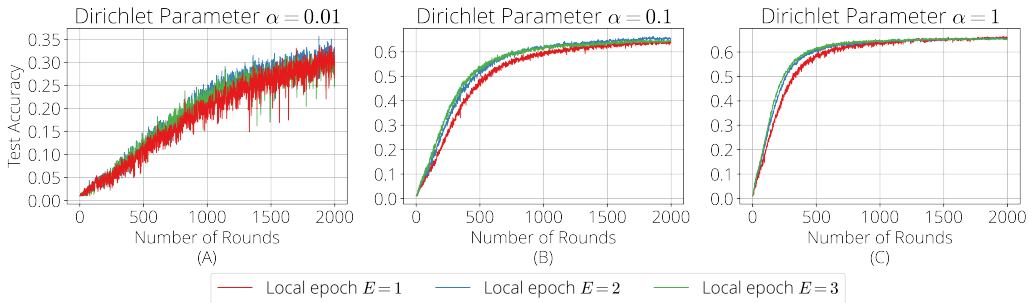


Figure 6

B.4 Additional experiments using different number of local data per client

In this subsection, we provide additional experimental results, where the size of the local dataset each client has differs. In particular, instead of distributing 500 samples to each client as done in Section 4 of the main text, we distribute $n_i \in [100, 500]$ samples for each client i , where n_i is the number of samples that client i has, and is randomly sampled from the range $[100, 500]$. We keep all other settings the same.

Then, in the server aggregation step (line 13 of Algorithm 1), we compute the weighted average of the local parameters, instead of the plain average, as suggested in [35], and used for instance in [47].

We experiment in two settings: CIFAR-10 dataset classification trained with a ResNet-18 [18], with Dirichlet concentration parameter $\alpha = 0.1$, which was the setting where the algorithms were fine-tuned using grid search; please see details in Section 4. We also provide results for CIFAR-100 dataset classification trained with a ResNet-50, with the same α .

The result can be found in Table 2. Similarly to the case with same number of data per client, *i.e.*, $n_i = 500$ for all $i \in [m]$, we see that Δ -SGD achieves good performance without any additional tuning. In particular, for CIFAR-10 classification trained with a ResNet-18, Δ -SGD achieves the second best performance after SGD (without LR decay), with a small margin. Interestingly, SGDM (both with and without LR decay) perform much worse than SGD. This contrasts with the same setting in Table 1, where SGDM performed better than SGD, which again complicates how one should tune client optimizers in the FL setting. For CIFAR-100 classification trained with ResNet-50, Δ -SGD outperforms all other methods with large margin.

<i>Non-iidness</i>	<i>Optimizer</i>	<i>Dataset / Model</i>	
Dir($\alpha \cdot \mathbf{p}$)		CIFAR-10	CIFAR-100
		ResNet-18	ResNet-50
$\alpha = 1$	SGD	80.7 _{↓(0.0)}	53.5 _{↓(4.0)}
	SGD (↓)	78.8 _{↓(1.9)}	53.6 _{↓(3.9)}
	SGDM	75.0 _{↓(5.7)}	53.9 _{↓(3.6)}
	SGDM (↓)	66.6 _{↓(14.1)}	53.1 _{↓(4.4)}
	Adam	79.9 _{↓(0.8)}	51.1 _{↓(6.4)}
	Adagrad	79.3 _{↓(1.4)}	44.5 _{↓(13.0)}
	SPS	64.4 _{↓(16.3)}	37.2 _{↓(20.3)}
	Δ -SGD	80.4 _{↓(0.3)}	57.5 _{↓(0.0)}

Table 2: Experimental results using different number of local data per client. Performance difference within 0.5% of the best result for each task are shown in **bold**. Subscripts_{↓(x.x)} is the performance difference from the best result and is highlighted in **pink** when the difference is bigger than 2%. The symbol (↓) appended to SGD and SGDM indicates step-wise learning rate decay, where the step sizes are divided by 10 after 50%, and another by 10 after 75% of the total rounds.